ANALYSIS OF THE LOWEST NATURAL FREQUENCIES OF HEAT EXCHANGER TUBES

By

WILLIAM TERRY LESTER

Bachelor of Science in Mechanical Engineering

Oklahoma State University

Stillwater, Oklahoma

1980

Submitted to the Faculty of the Graduate College
of the Oklahoma State University
in partial fulfillment of the requirements
for the Degree of
MASTER OF SCIENCE
May, 1982

ANALYSIS OF THE LOWEST NATURAL FREQUENCIES

OF HEAT EXCHANGER TUBES

Thesis Approved:

R L Lowery
Thesis Adviser

P M Moretti

J. K. Good

Norman N Durham
Dean of the Graduate College

PREFACE

The objective of this thesis was to find the lowest three natural frequencies of heat exchanger U-tubes by numerical and experimental methods. The results were transformed into a usable form for a heat exchanger design engineer.

I would like to thank my major adviser, Dr. Richard L. Lowery, for the help, advice, and guidance he has given me. Also, appreciation is extended to the other committee members, Dr. Peter M. Moretti and Mr. Keith Good, for the advice and assistance they so freely gave. I also appreciate the suggestions and assistance of Bill Hobson and George Cooper.

Finally, I would like to thank my mother and father, Nova and Wilbur Lester, for the love they have given to me.

TABLE OF CONTENTS

LIST OF FIGURES

LIST OF SYMBOLS

A	cross sectional area
E	Young's modulus of elasticity
f	natural frequency Hz
F	forces
k_{ij}	stiffness
L	span length
L_o	overhang length
m_{ij}	mass
M	moments
r_j	moment arm
R_k	constraint reaction forces
T_k	constraint reaction
x_j	mode shape
α	dimensionless frequency
δ_{SL}	maximum deflection of span lengths
δ_{SS}	maximum deflection of semicircular section
π	pi, 3.1416
μ	mass per unit length of tube
ω	natural frequency radians per second

CHAPTER I

INTRODUCTION

The analysis of the lowest natural frequencies of heat exchanger U-tubes was done to prolong the life of the heat exchanger by eliminating failures caused by low stress fatigue. The vibration of the U-tube is the prime cause of the low stress fatigue. The worst vibrations occur when the U-tube goes into resonance. The U-tube will go into resonance when the frequency of the excitation force is equivalent to a natural frequency.

The vibration of the U-tube is reduced by increasing the difference between excitation frequencies on the natural frequencies of the U-tubes. To increase the difference between the excitation frequency and the natural frequency in the design stage, the excitation frequency needs to be known. Then the U-tube can be designed to have a desired natural frequency.

In this analysis the lowest three natural frequencies for several U-tube configurations were found by numerical and experimental methods. The numerical analysis was done with the generalized finite element program called NASTRAN. For each U-tube configuration model with NASTRAN, the lowest three natural frequencies and the corresponding mode shapes were determined.

In the experimental analysis the lowest three natural frequencies of several U-tube geometries were measured. The natural frequencies

were found by slowly varying the frequency of the excitation force applied to the U-tube. When the excitation frequency was a natural frequency, the U-tube would go into resonance. With the U-tube in resonance a natural frequency was found.

The natural frequencies obtained from the numerical and experimental analyses were transformed into a more usable form. The results from the numerical and experimental analyses were compared to verify the results and explain the observations.

From a search of alternative methods for finding the natural frequencies, a modified version of Holzer's method was found. This version of Holzer's method can be applied to any spring-mass system.

CHAPTER II

NUMERICAL ANALYSIS

The first three natural frequencies of the U-tube configurations shown in Figure 1 were determined analytically with NASTRAN, which is a generalized finite element computer program that can solve a wide range of problems from heat conduction to solid mechanics. Level 15.5 Cosmic is the version of NASTRAN used at Oklahoma State University.

To find the natural frequency of a U-tube configuration, NASTRAN was given the geometry and material properties of the configuration. NASTRAN would then generate the mass and stiffness matrix of the configuration which changed the problem into an eigenvalue problem.

With NASTRAN a variety of methods can be used to find the eigenvalues. The method used was the inverse method in which the inverse of the stiffness was taken. Then the desired eigenvalues were determined by a method similar to the power series method.

The U-tube configurations in Figure 1 consisted of single, double, triple, and quadruple span geometries with all pin connections and the quadruple span with the ends clamped. For these configurations the radius of the semicircular section R over the span length L varied from 1/8 to 1. For all of the analytical analysis, the span length was 24 in. The area moment of inertia I was 0.03355 $in.^4$. Young's modulus of elasticity E was 30.0×10^6 $lbf/in.^2$. The mass per unit length of the tube μ was 251.0×10^{-6} $lbf \cdot sec^2/in.^2$.

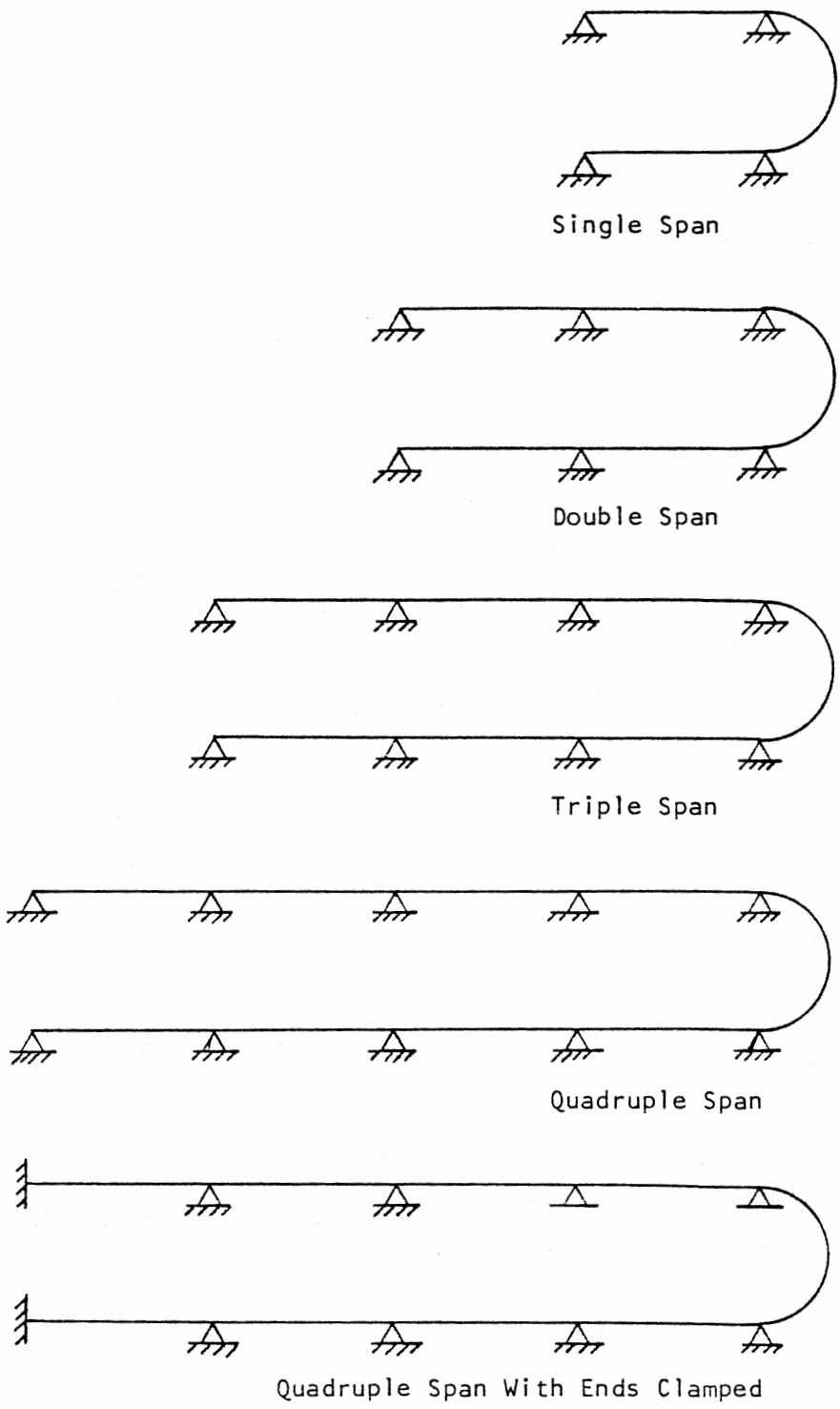

Figure 1. Configurations Used With NASTRAN

Each U-tube configuration was modeled with straight bar elements. All span lengths were divided into 12 elements of equal length. Each semicircular section of the U-tube consisted of 36 elements. Each of these elements represented an arc of 5 degrees of the semicircular section.

To obtain good results with NASTRAN, the size difference of the elements should not be greater than 10 to 1. The largest difference was 8 to 1; this occurred when R/L was 1/8.

The mode shapes of the three lowest natural frequencies were the first out-of-plane mode, the second out-of-plane mode, and the first in-plane mode, as shown in Figures 2, 3, and 4. For the out-of-plane modes the major displacements occurred in the direction normal to the plane in the direction normal to the plane in which the U-tube lay. The first out-of-plane mode was shaped similarly to a continuous sine wave with all the nodes at the pin or clamp connections; the opposite span lengths were in phase.

The second out-of-plane mode was shaped similarly to a continuous sine wave with one node at the outer tip of the semicircular section, and the remaining nodes at the pin and clamp connections. The additional node and opposite spans were out of phase by 180 degrees. The major displacements of the in-plane modes occurred in the plane in which the U-tube lay.

The first in-plane mode shape was also similar to a continuous sine wave with all nodes at the pin or clamp connections. All displacements occurred in the plane in which the U-tube lay. Again the opposite span lengths were in phase.

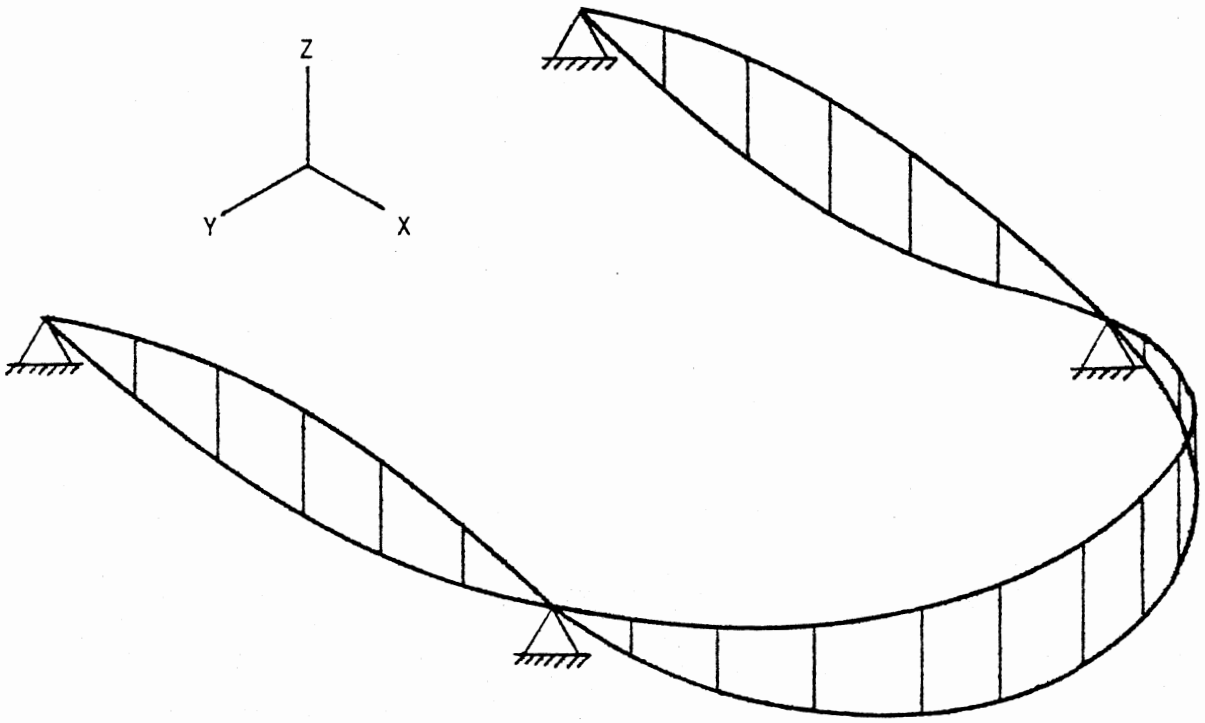

Figure 2. First Out-of-Plane Mode: Full Span Deflection and all Major Deflections Occur in the Y Direction

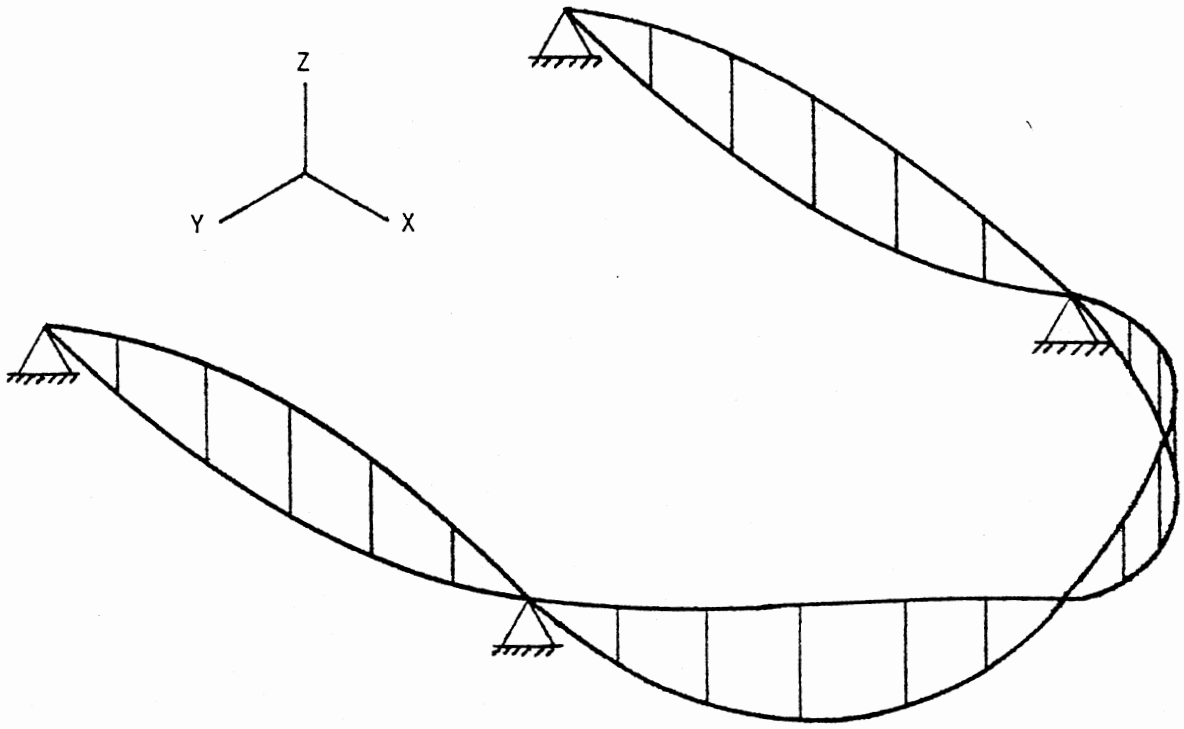

Figure 3. Second Out-of-Plane Mode. Full Span Deflection and all Major Deflections Occur in the Z Direction

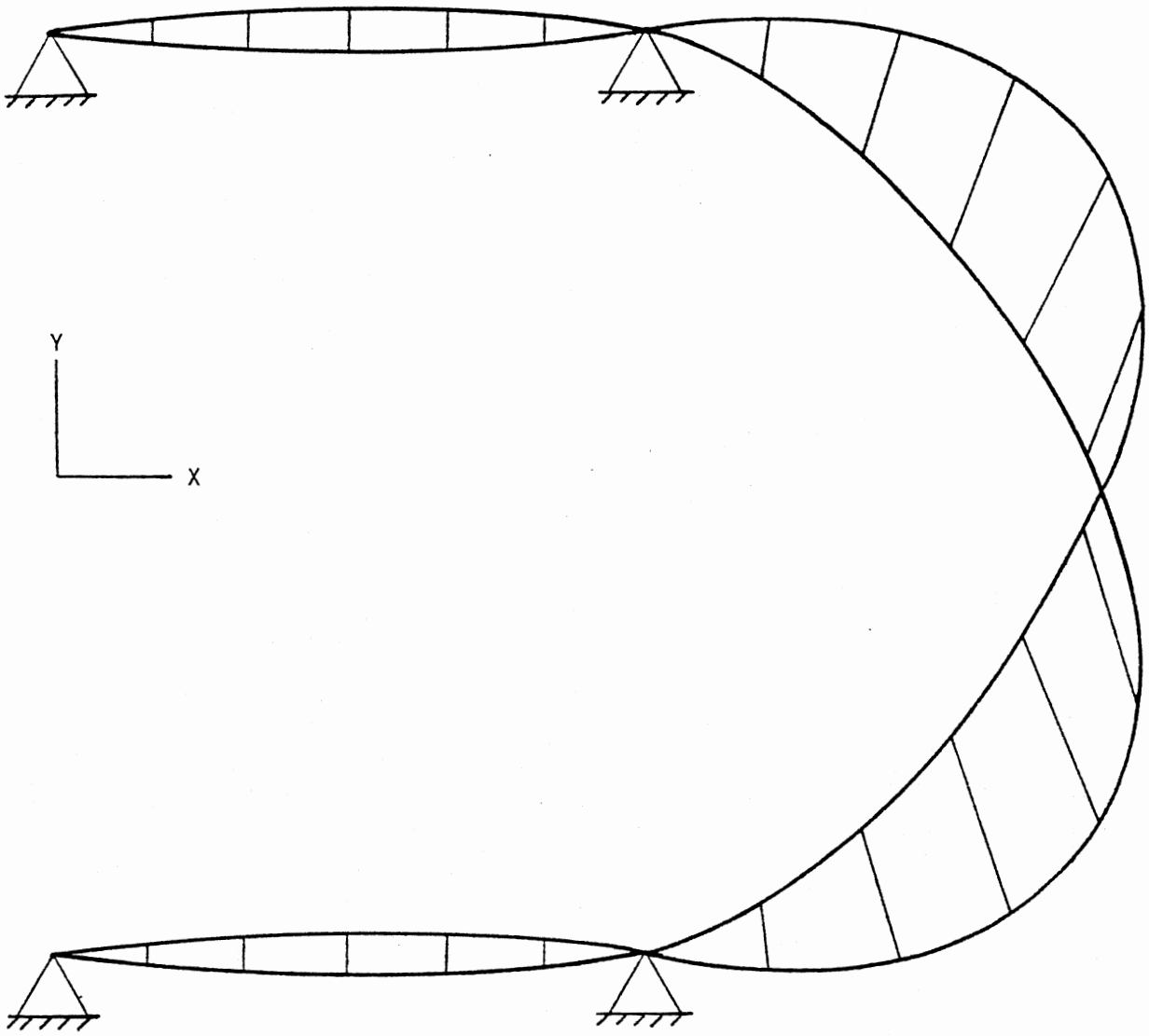

Figure 4. First In-Plane Mode: Full Span Deflection and all Deflections Occur in the X-Y Plane

These three natural frequencies from the NASTRAN computer runs are tabulated in Appendix A. The frequencies were constrained by material properties, geometry of the cross section of the tube, span length, and radius of the semicircular section. To make the data more versatile the frequencies were transformed into a dimensionless variable α by Equation (1). Thus α is dependent on R/L and independent of the material properties and the cross sectional geometry.

$$\alpha = 2\pi f L^2 \left[\frac{\mu}{IE}\right]^{1/2}$$

or

$$f = \frac{\alpha}{2\pi L^2} \left[\frac{IE}{\mu}\right]^{1/2} \qquad (1)$$

The values of α versus R/L from Appendix A were plotted in Figures 5 through 8. Figure 5 shows the first out-of-plane mode with all pin connections. The double, triple, and quadruple spans virtually lay on the same curve. The single span has the same shape but is offset from the other curves by a fraction. At R/L equal to 1, all four configurations have the same value of α and the curves tend to separate as R/L approaches 1/4. Basically the first out-of-plane mode shape within the range of 1/4 to 1 was independent of the number of span lengths.

In Figure 6, α versus R/L was plotted for the second out-of-plane mode with all pin connections. At R/L equal to 1/2, the values of α are similar and the slopes tend to converge as R/L approaches 1. Between R/L equal to 1/4 and 1/2, the slopes of all four configurations cross and produce slopes in four independent directions. If the plots were continued to zero, the single span configuration would behave like a

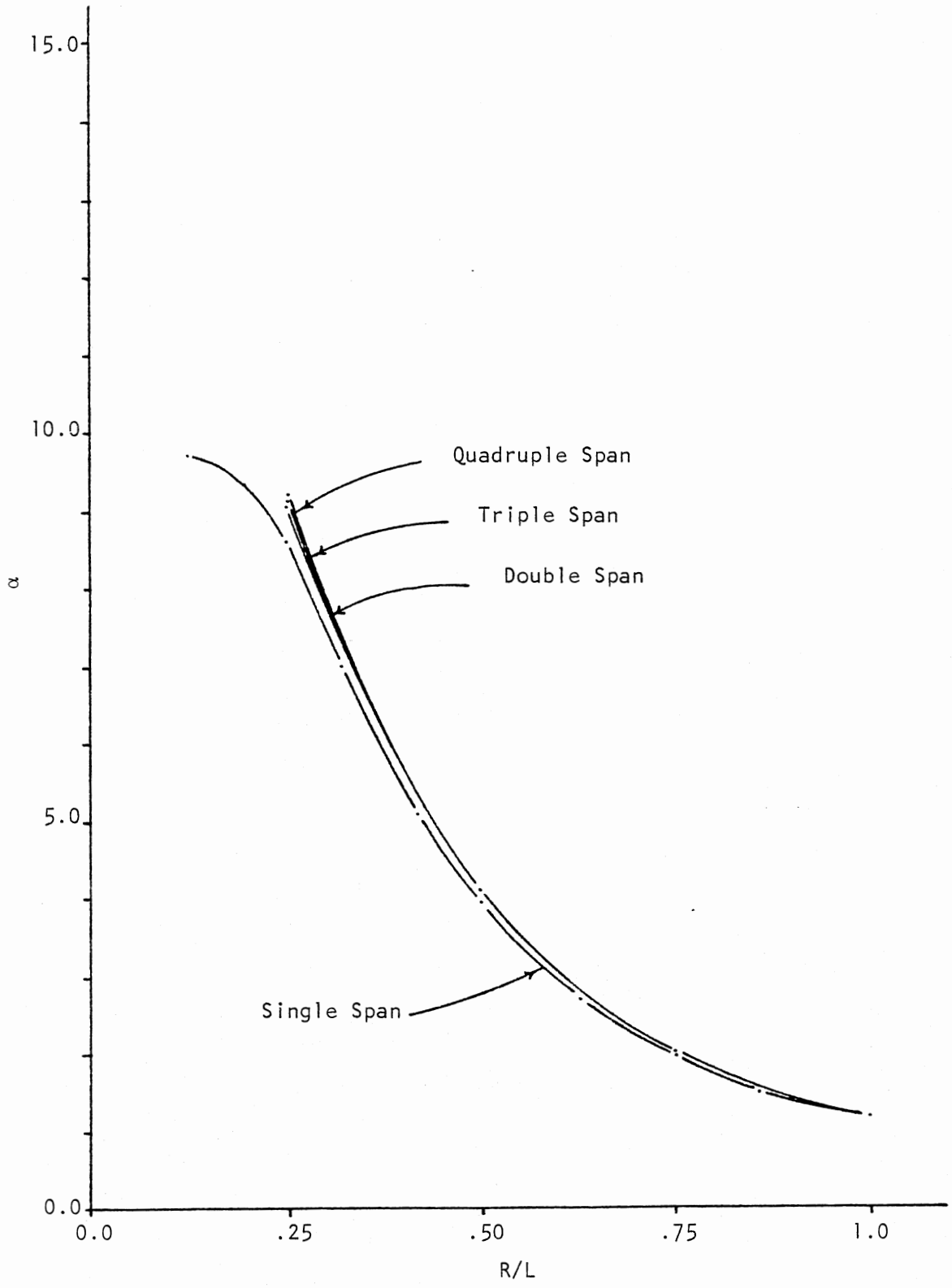

Figure 5. First Out-of-Plane Mode (α vs. R/L)

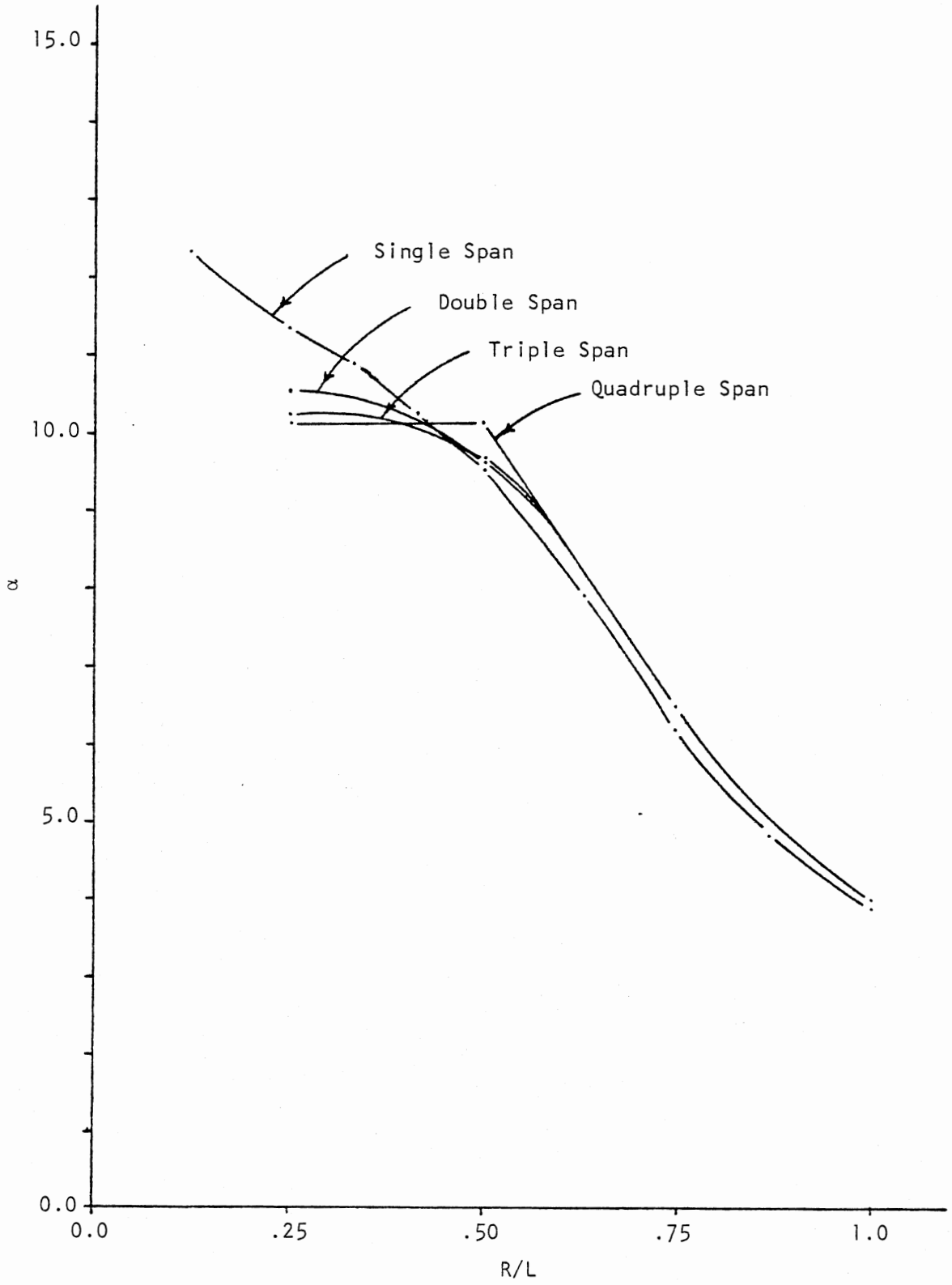

Figure 6. Second Out-of-Plane Mode (α vs. R/L)

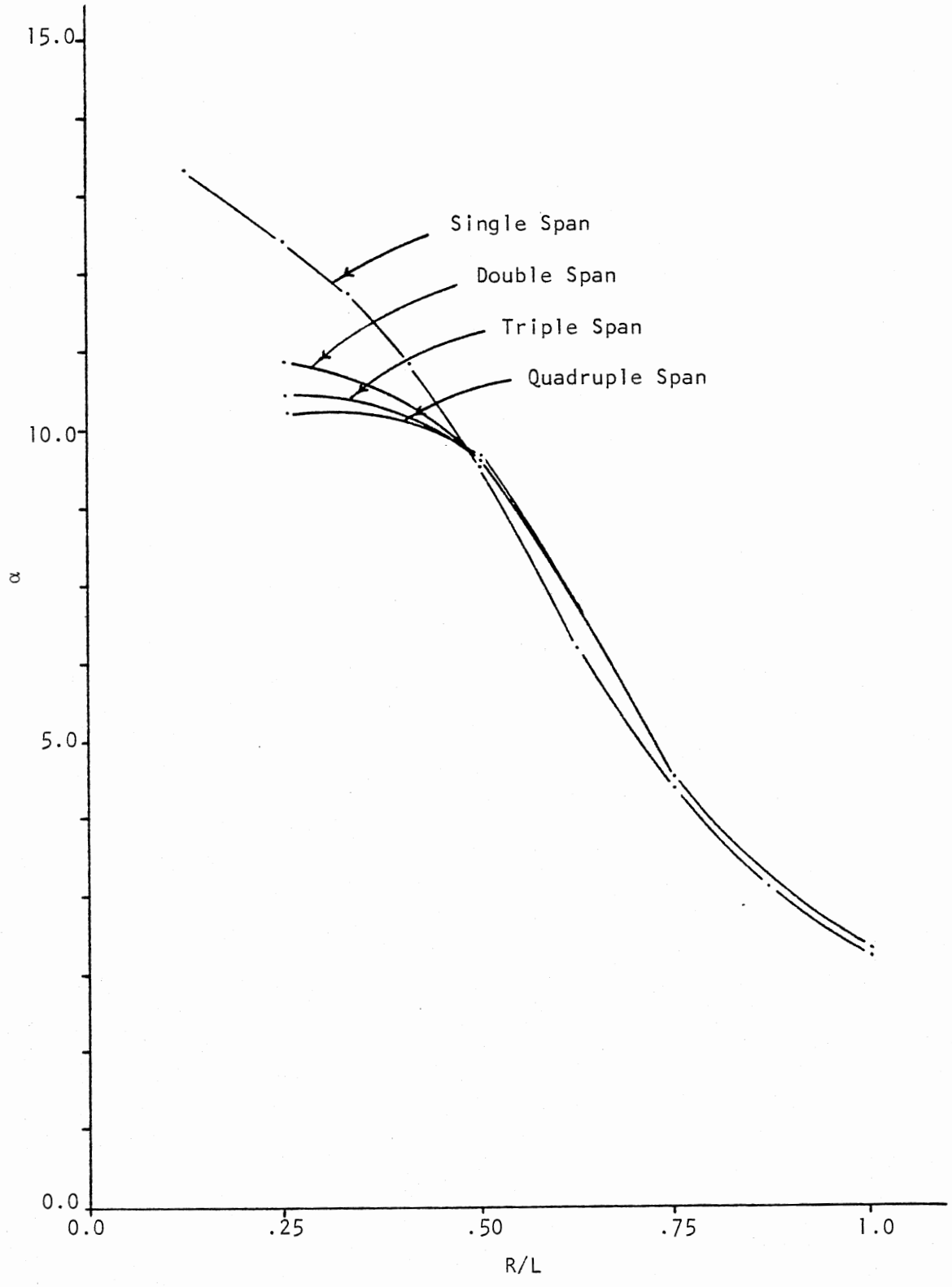

Figure 7. First In-Plane Mode (α vs. R/L)

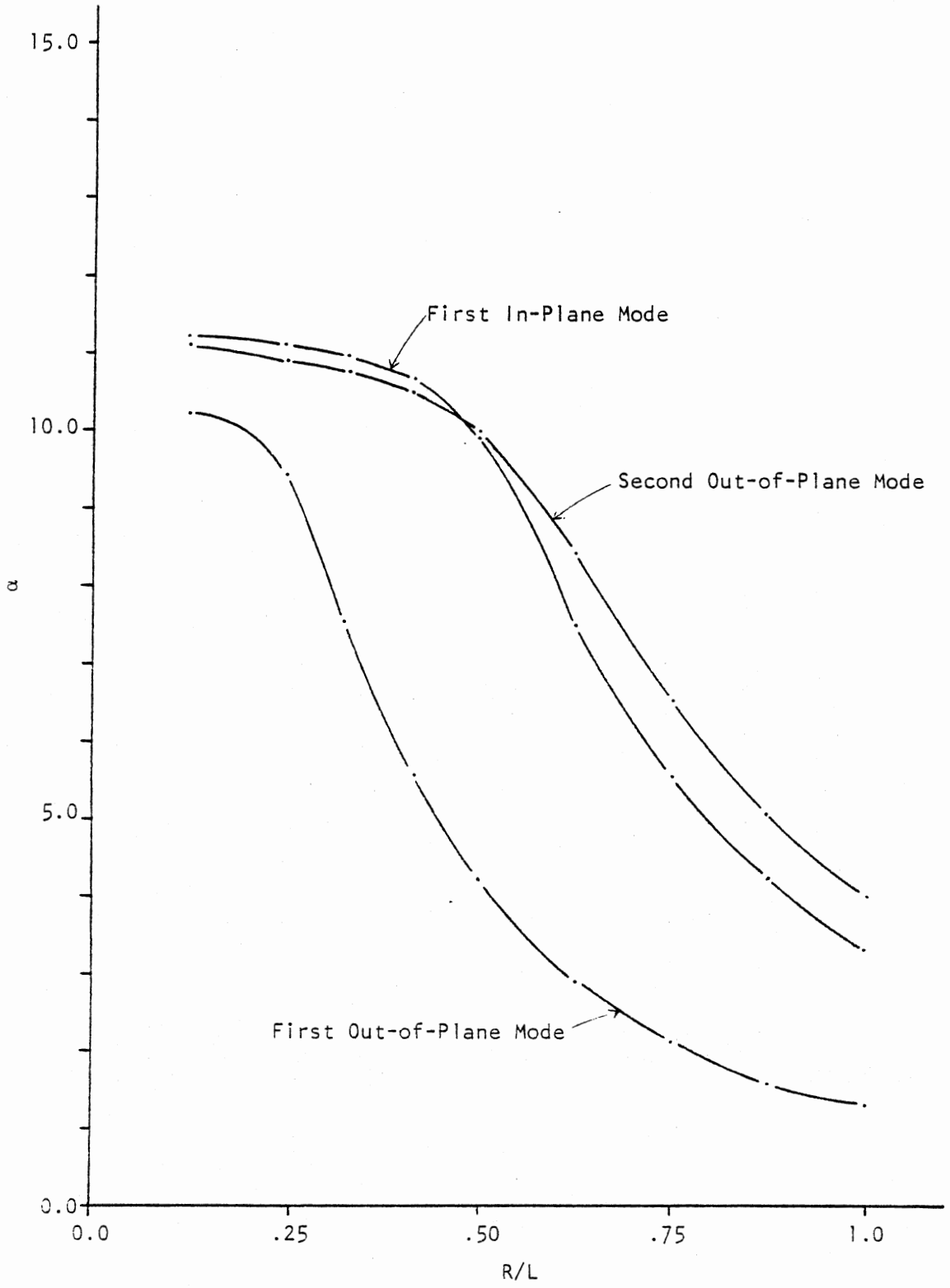

Figure 8. Quadruple Span With Ends Clamped (α vs. R/L)

pin-clamp beam, while the quadruple span would behave like a pin-pin-pin-pin-clamp beam and would have a lower natural frequency than the single span.

In Figure 7, the values of α for the first in-plane mode shape with all pin connections were plotted. These results were almost the same as the second out-of-plane mode data in Figure 6. The first in-plane results were lower within the range R/L equal to 1/2 and 1, and higher within the range R/L equal to 1/4 to 1/2. These results also generated smoother curves than those in Figure 6.

The values of α for the first three modes of the quadruple span with ends clamped are plotted in Figure 8. The results were similar in shape to the slopes but were slightly higher than the results from the pinned configurations. Except for the R/L range from 1/4 to 1/2, the values of the first in-plane and second out-of-plane modes were between the values of α for the single and double spans on all pin connection configurations.

Each natural frequency of a U-tube configuration has a particular mode shape. When a U-tube is excited with one of its natural frequencies, it must vibrate in the particular mode shape of the natural frequency. It will not vibrate in some random pattern. This would indicate a strong bond of a natural frequency and its mode shape with the maximum potential energy and the maximum kinetic energy of a given U-tube configuration.

The maximum potential energy and the maximum kinetic energy are dependent on the displacement of the mode shape along the U-tube for a given natural frequency. Therefore, the ratio of the maximum deflection along the span length over the maximum deflection along the semicircular section would be an indicator of how the maximum potential energy and the maximum kinetic energy was distributed along the U-tube.

The mode shape was generated for each natural frequency produced with NASTRAN. With these mode shapes, the ratio of the maximum deflection along the span length δ_{SL} over the maximum deflection along the semicircular section δ_{SS}. These ratios were rough indicators of how much energy was stored along the span lengths and the semicircular sections of the U-tube.

For Figures 9, 10, 11, and 12, δ_{SL}/δ_{SS} was plotted for the corresponding plots of α versus R/L in Figures 5, 6, 7, and 8. The values of δ_{SL}/δ_{SS} are tabulated in Appendix B. Comparing the plots of α versus R/L and δ_{SL}/δ_{SS}, the general shape and relationship of the curves of these plots were the same. These plots firmly emphasize a strong bond between natural frequency, mode shape, maximum potential energy, and maximum kinetic energy of the U-tube.

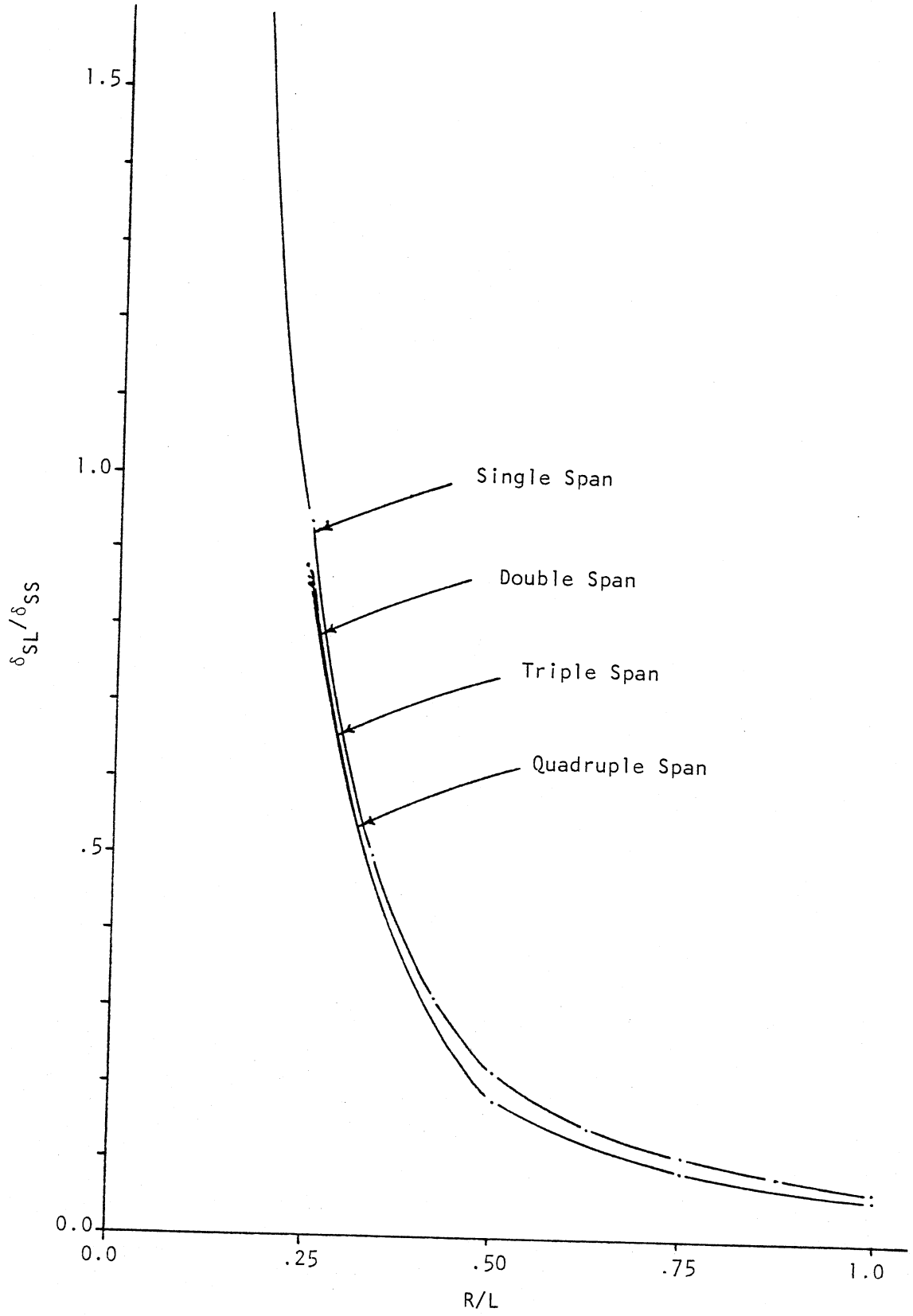

Figure 9. First Out-of-Plane Mode (δ_{SL}/δ_{SS} vs. R/L)

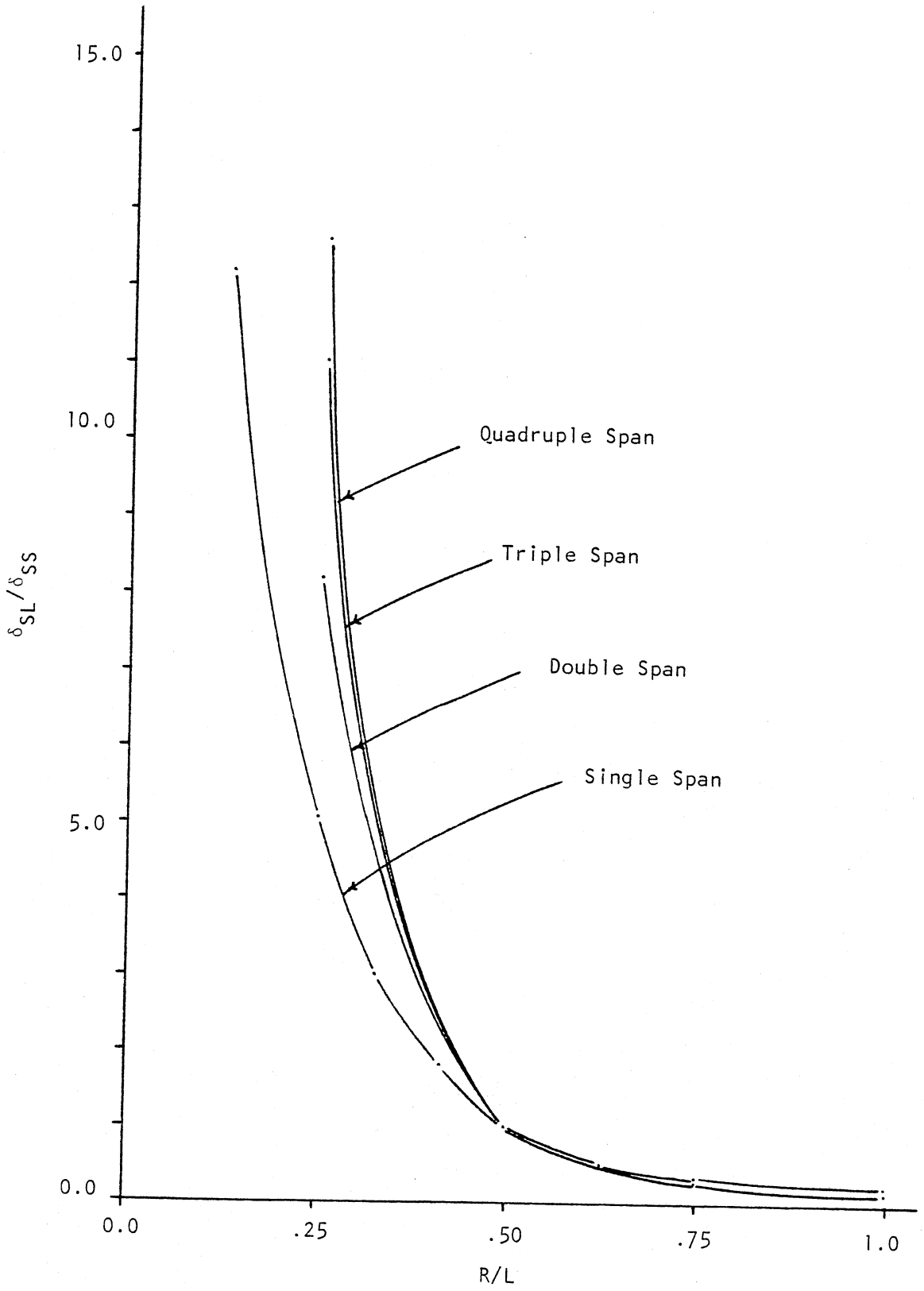

Figure 10. Second Out-of-Plane Mode (δ_{SL}/δ_{SS} vs. R/L)

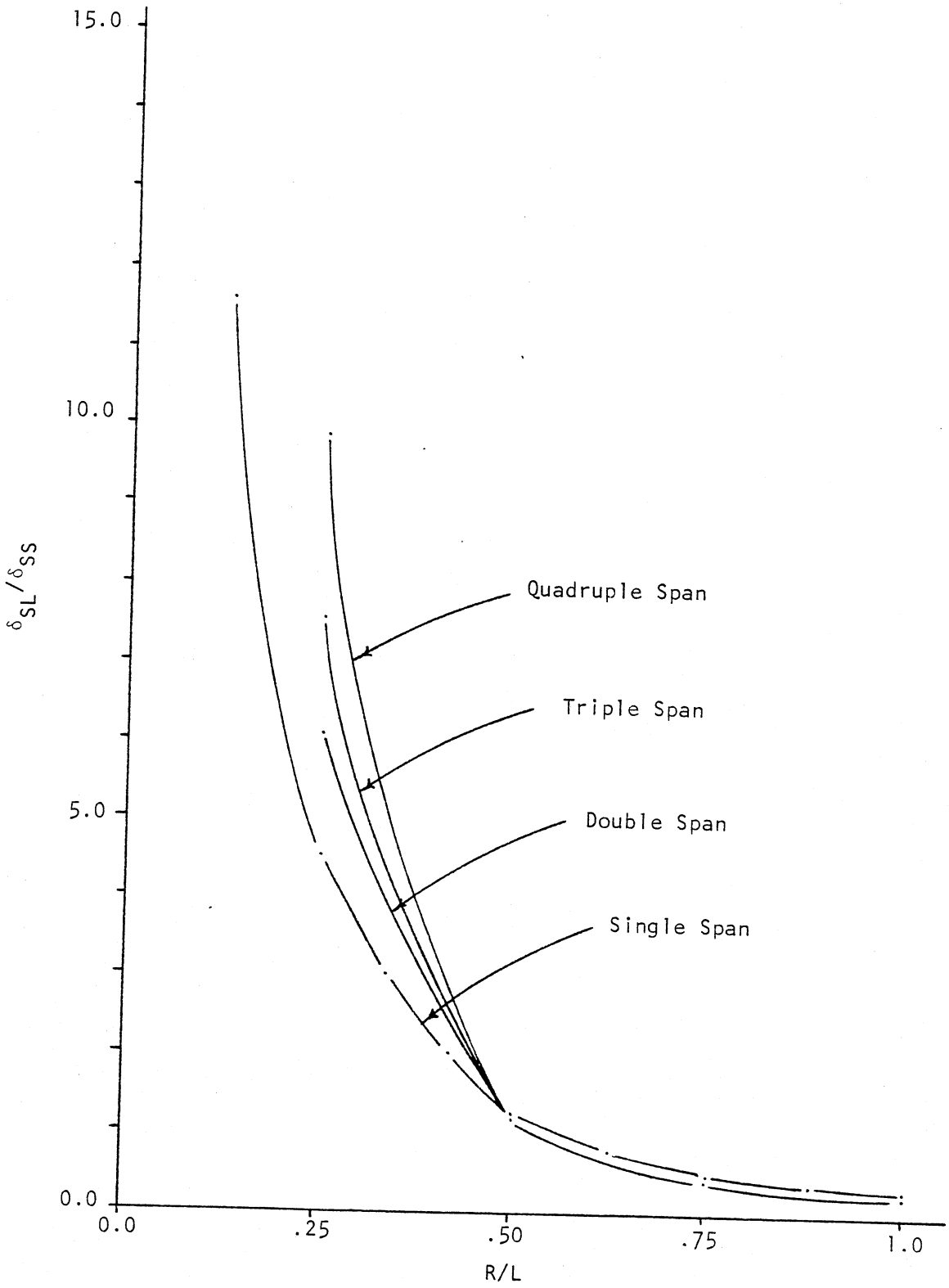

Figure 11. First In-Plane Mode (α vs. R/L)

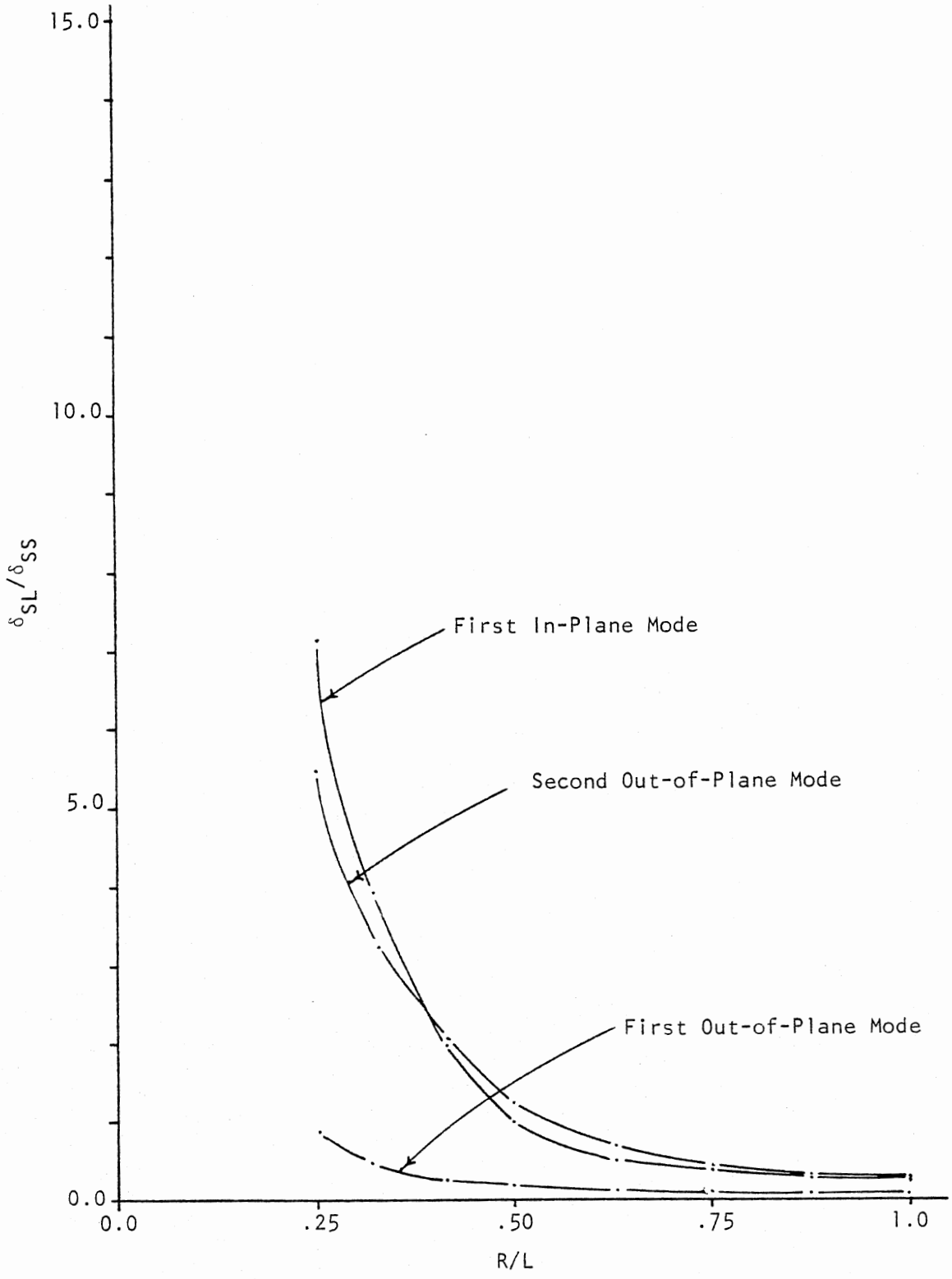

Figure 12. Quadruple Span With Ends Clamped (δ_{SL}/δ_{SS} vs. R/L)

CHAPTER III

EXPERIMENTATION

The experimentation was done on two U-tubes of 12.0- and 12.5-inch radii. The three lowest natural frequencies were measured for the quadruple span configuration with the ends clamped. Measurements were taken with the ratio of the semicircular section radius R over the span length L ranging from 1/4 to 1. Also, for each configuration the three lowest natural frequencies were measured with the overhang length L_o ranging from 0 to 24 in. The overhang length is shown in Figure 13.

The measurements were taken by the instrumentation schematic shown in Figure 14. Shown in Figure 15 are the audio oscillator, the universal counter, and the dual beam oscilloscope that were used. The audio oscillator generated the excitation signal, the universal counter determined the frequency being generated by the audio oscillator, and the dual beam oscilloscope was used to get the Lissajous patterns of the signal from the audio oscillator versus the response of the U-tube. The response of the U-tube was obtained with the two piezoelectric accelerometers. One of the accelerometers is shown in Figure 16.

Along the U-tube the excitation force was applied with the two electromagnets shown in Figure 17. One electromagnet received the positive half of the signal from the audio oscillator; the other electromagnet received the negative half of the signal. The signal from the audio oscillator was split with four diodes. The U-tubes were excited in this manner, so only one mode at a time would be excited.

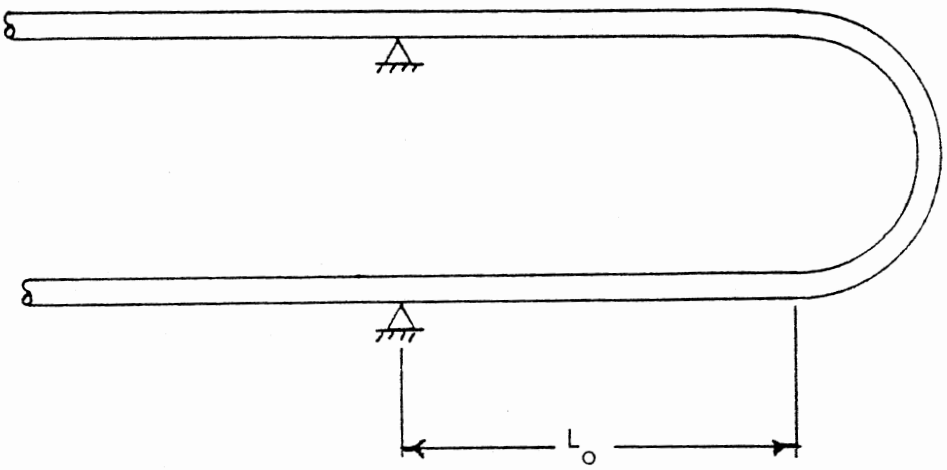

Figure 13. Overhang Length (L_o), Length From the End of the Semicircular Section to the First Pin Connector

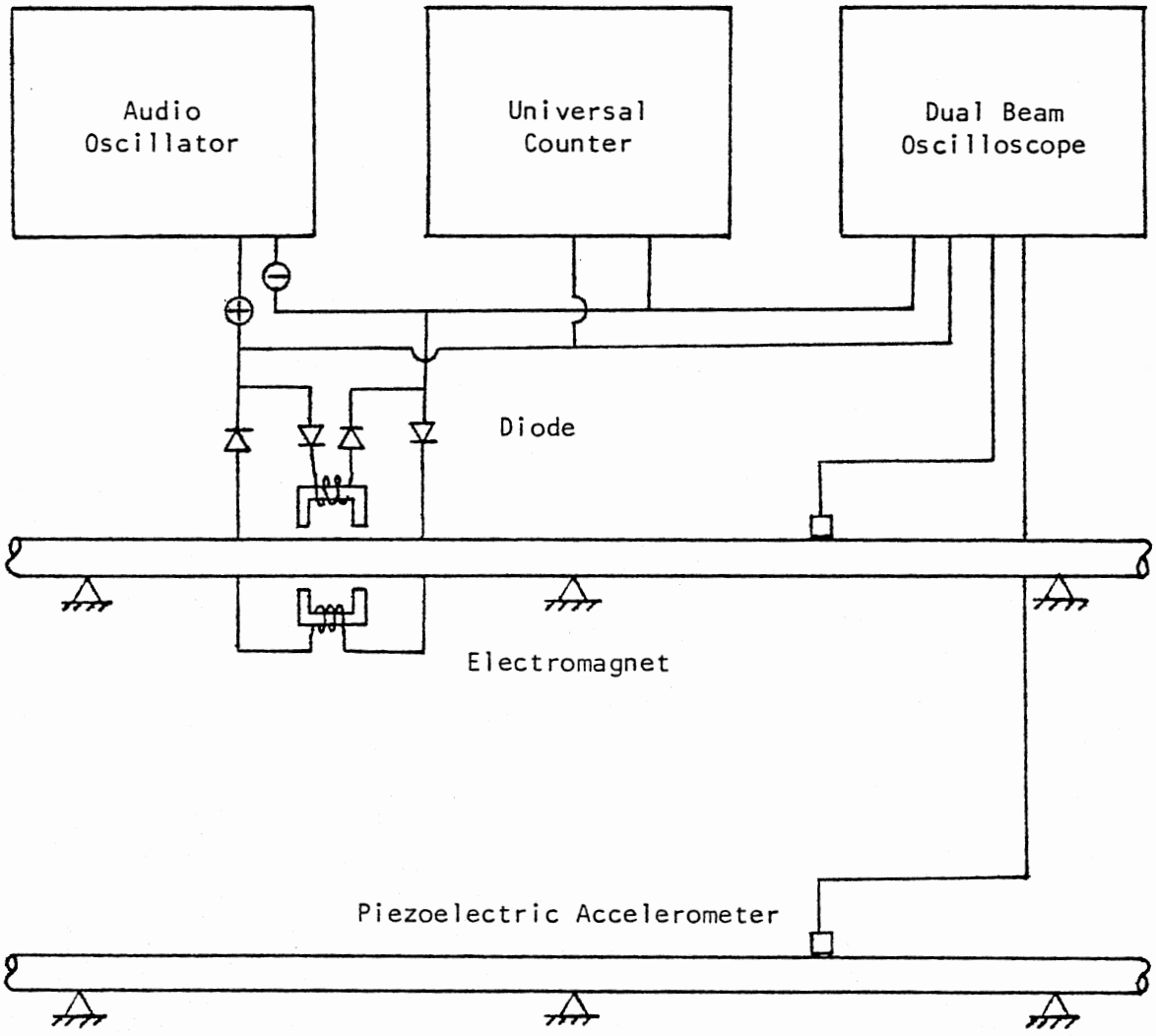

Figure 14. Instrumentation Schematic

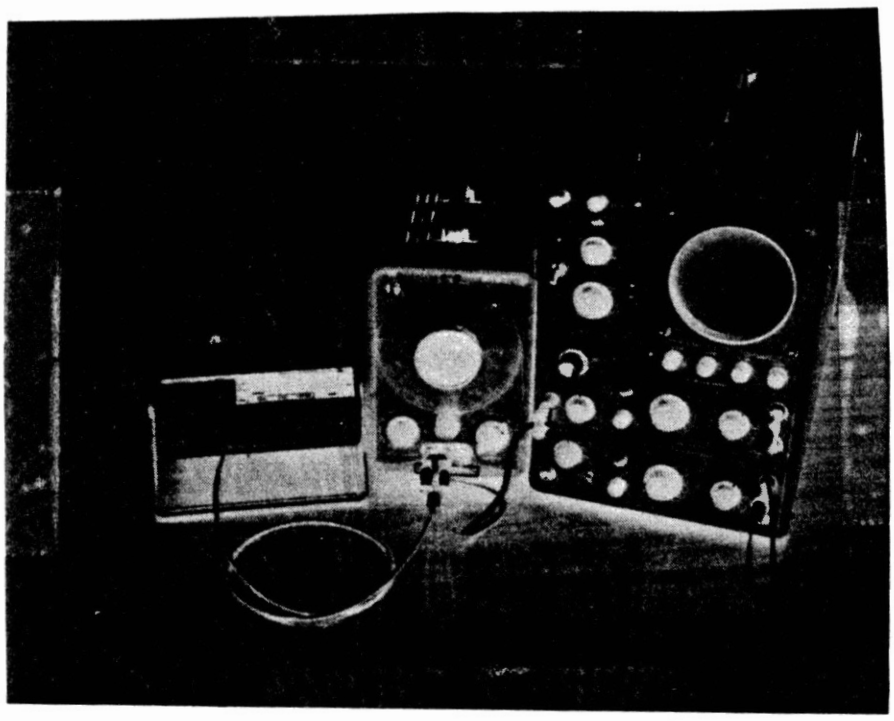

Figure 15. The Oscilloscope, Audio Oscillator, and Universal Counter Used in the Experiment

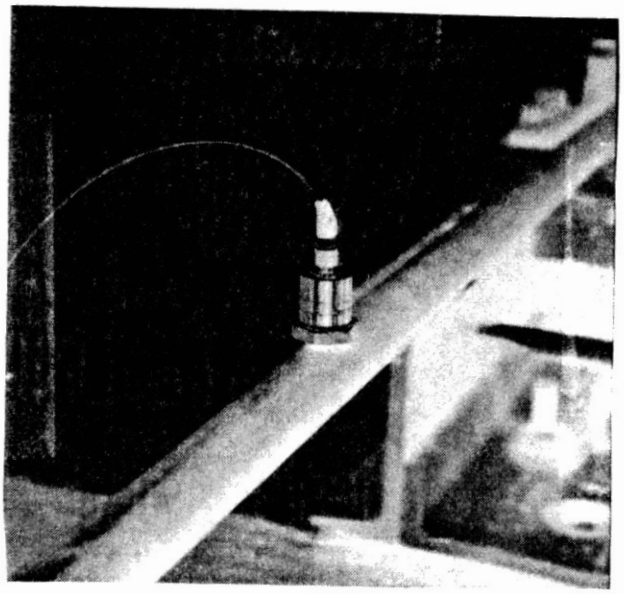

Figure 16. The Piezoelectric Accelerometer Glued With Super Glue to the U-Tube

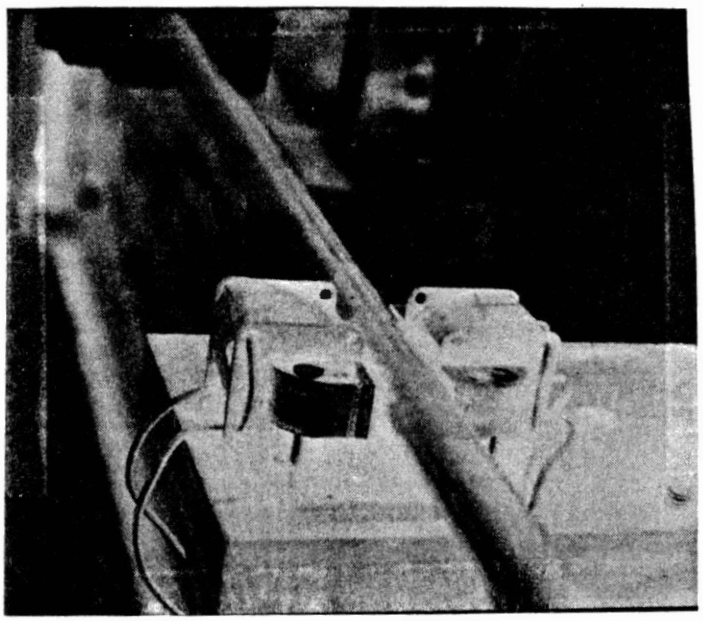

Figure 17. Electromagnets Used to Apply the Excitation Force

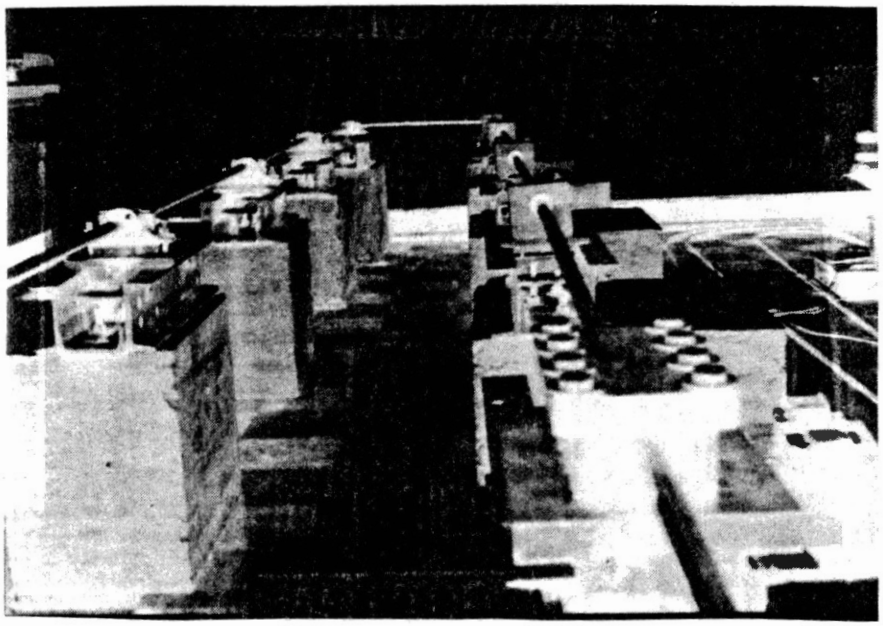

Figure 18. U-Tube and Test Bench

At the natural frequencies the Lissajous patterns of the excitation signal versus the response of the U-tube was a 1-to-1 pattern. When the excitation signal was a natural frequency, 1-to-1 Lissajous patterns of the excitation signal versus the response of the U-tube were generated on the dual beam oscilloscope.

After a natural frequency was found, the phase angle of opposite span lengths was determined to check the mode shape. Since the opposite span lengths are in phase for the first out-of-plane and first in-plane modes, and the opposite span lengths are out of phase by 180 degrees for the second out-of-plane and second in-plane modes, the check was done by changing the setting on the oscilloscope from its Lissajous pattern to its real time mode. The display on the oscilloscope would be two sine waves. If the sine waves correspond to each other, the opposite span lengths were in phase. If the sine waves were out of phase by 180 degrees, the opposite span lengths were out of phase by 180 degrees.

The U-tubes were constrained with the test bench in Figure 18. The test bench consisted of ten 300-pound concrete blocks with anchor bolts. The anchor bolts secured a piece of channel iron to each block. The pinned and clamped connectors were clamped to the channel iron with two bolts through additional pieces of channel iron.

The pinned connector shown in Figure 19 was similar to a split journal bearing which held a piece of bar stock in place. A hole was drilled into the bar stock the diameter of the U-tube. The bar stock was bored so that a thickness of 1/8 inch of the hole drilled through the bar stock was in contact with the U-tube.

The clamped connector in Figure 20 has a piece of bar stock that was bored to the diameter of the U-tube and then split. The two halves of

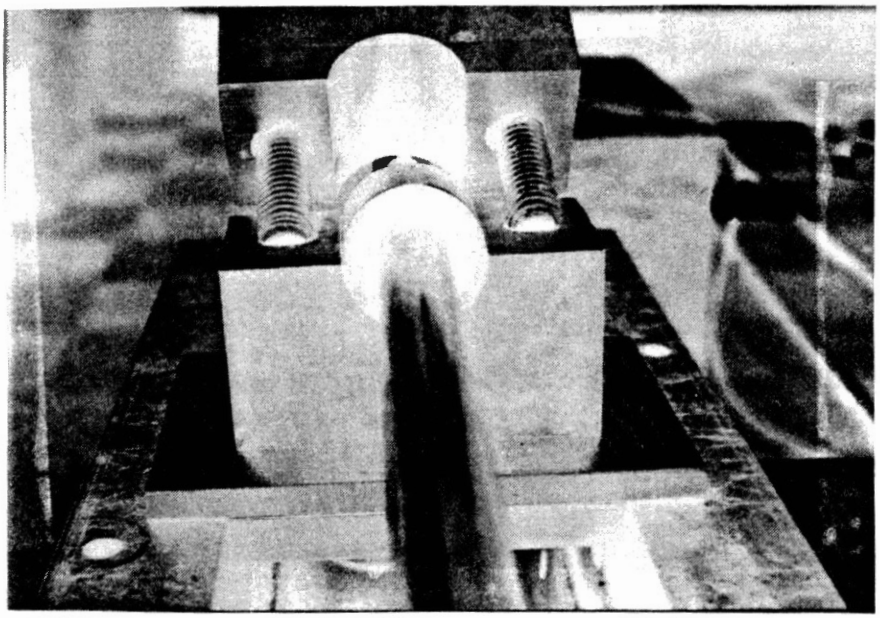

Figure 19. Pinned Connector Which Applied a Pin Connection to the U-Tube

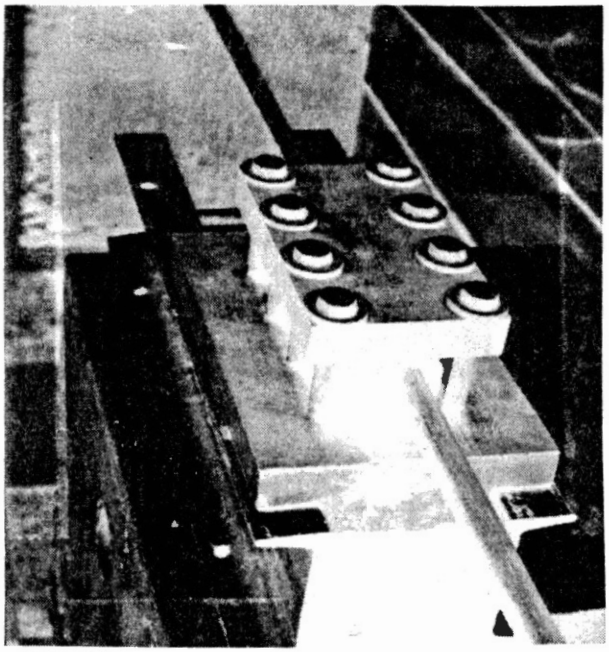

Figure 20. Clamped Connector Which was an Effective End Clamp

the bar stock were placed around a section of the U-tube and pressed between two plates. The plates were pulled together with eight bolts.

The clamped connector was an effective end clamp. The vibration of the U-tube on one side of the connection was not transmitted through the connection to the section of the U-tube on the other side of the clamped connection.

The natural frequencies obtained from the experimentation were constrained by material properties, geometry of the cross section, span length, and radius of the semicircular section. Like the natural frequencies obtained from the numerical analysis, the natural frequencies from the experimentation were also transformed to a dimensionless value α with Equation (1). These natural frequencies and corresponding values of α are tabulated in Appendix C.

In Equation (1) the value of the square root of Young's modulus of elasticity times area moment of inertia divided by the mass per unit length of tube $\sqrt{EI/\mu}$ used for the experimentation was also found through experimentation. Since $\sqrt{EI/\mu}$ was a constant for all of the U-tube, $\sqrt{EI/\mu}$ was determined for a 2-foot section of the U-tube. The first natural frequency of the 2-foot section with a free-free beam configuration was found with a real-time spectral analyzer. The frequency was 306 Hz. From Reference (1), α was 22.4 free-free beam configuration. Therefore, $\sqrt{EI/\mu}$ was 7670.0 radians per second.

Shown in Figure 21 is the plot of α versus R/L for the first out-of-plane, second out-of-plane, and first in-plane modes. This plot is similar to Figure 8, with the exception that the second out-of-plane and first in-plane modes did not intersect.

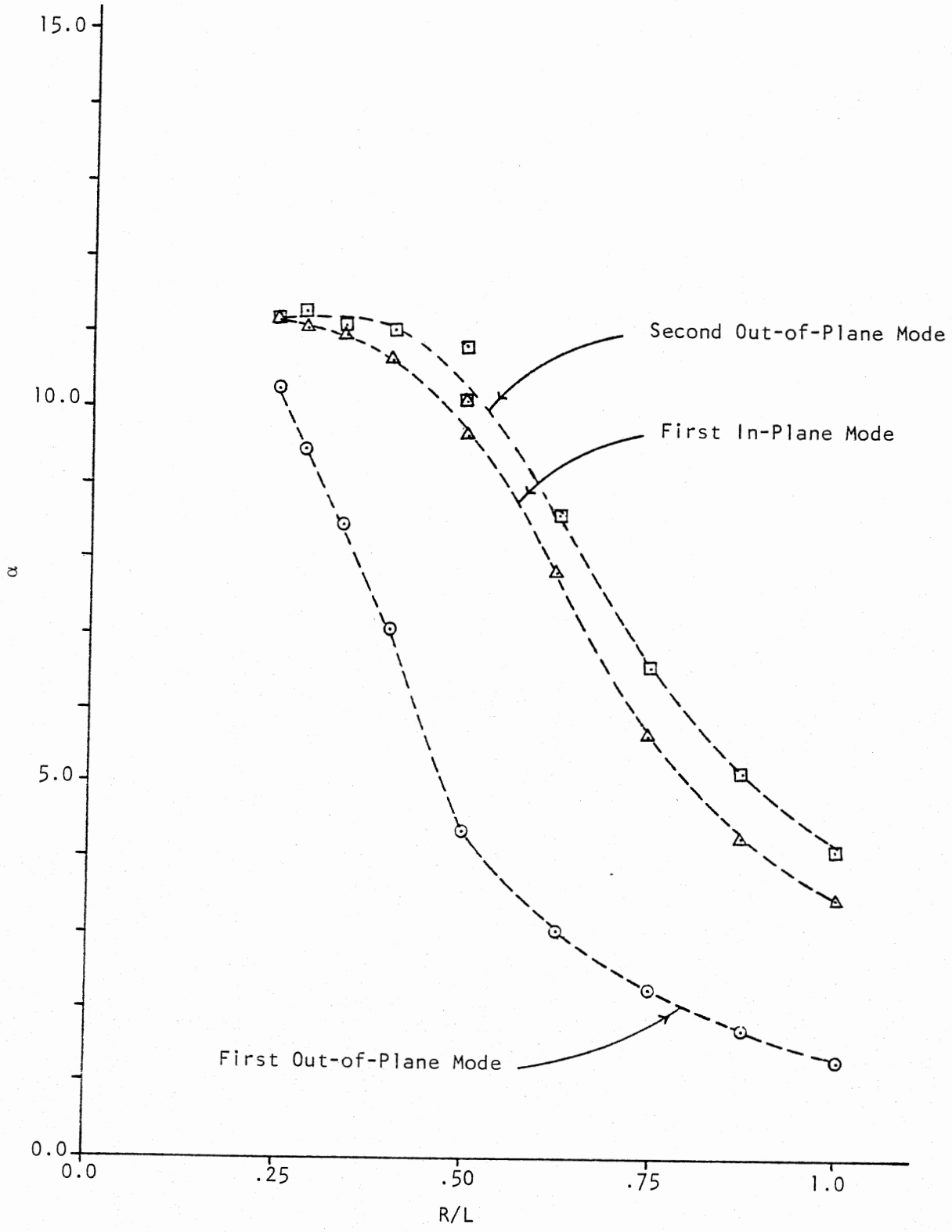

Figure 21. α vs. R/L

In Figures 22, 23, and 24, α versus L_o/L was plotted for the first out-of-plane, second out-of-plane, and first in-plane modes. The plots show the sensitivity in the change of α for a change in L_o/L for corresponding values of R/L. The maximum change of α for L_o/L ranging from 0.0 to 0.2 was 40 percent. This occurred in the first out-of-plane mode with R/L equal to 2/5.

All measurements were rounded to the nearest Hz; therefore, no additional errors were caused by the instrumentation. The percent error produced by the resolution of half a Hz was dependent on the frequency of the measurement taken. The maximum percent error produced by the half-Hz resolution was 3 percent of the value of α.

From mounting the U-tube on the test bench, there was a $\pm 1/4$ of an inch error. This would cause a 4 percent error in the value of α. This error, combined with the error from rounding off to the nearest Hz,would cause a maximum 7 percent error in the experimental values of α.

To find the effectiveness of applying a force normal to the span lengths and bending moments of one of the pin connections, a test bench block was moved normal to the span lengths. The force and bending was applied to several R/L ratios. For all cases the force and bending moments caused no noticeable change of the lowest three natural frequencies.

To excite a natural frequency, the excitation force has to be applied in the direction of the displacements of the mode shapes. If the excitation force was applied normal to the displacement directions of the mode shape for a given natural frequency, the U-tube would not go into resonance.

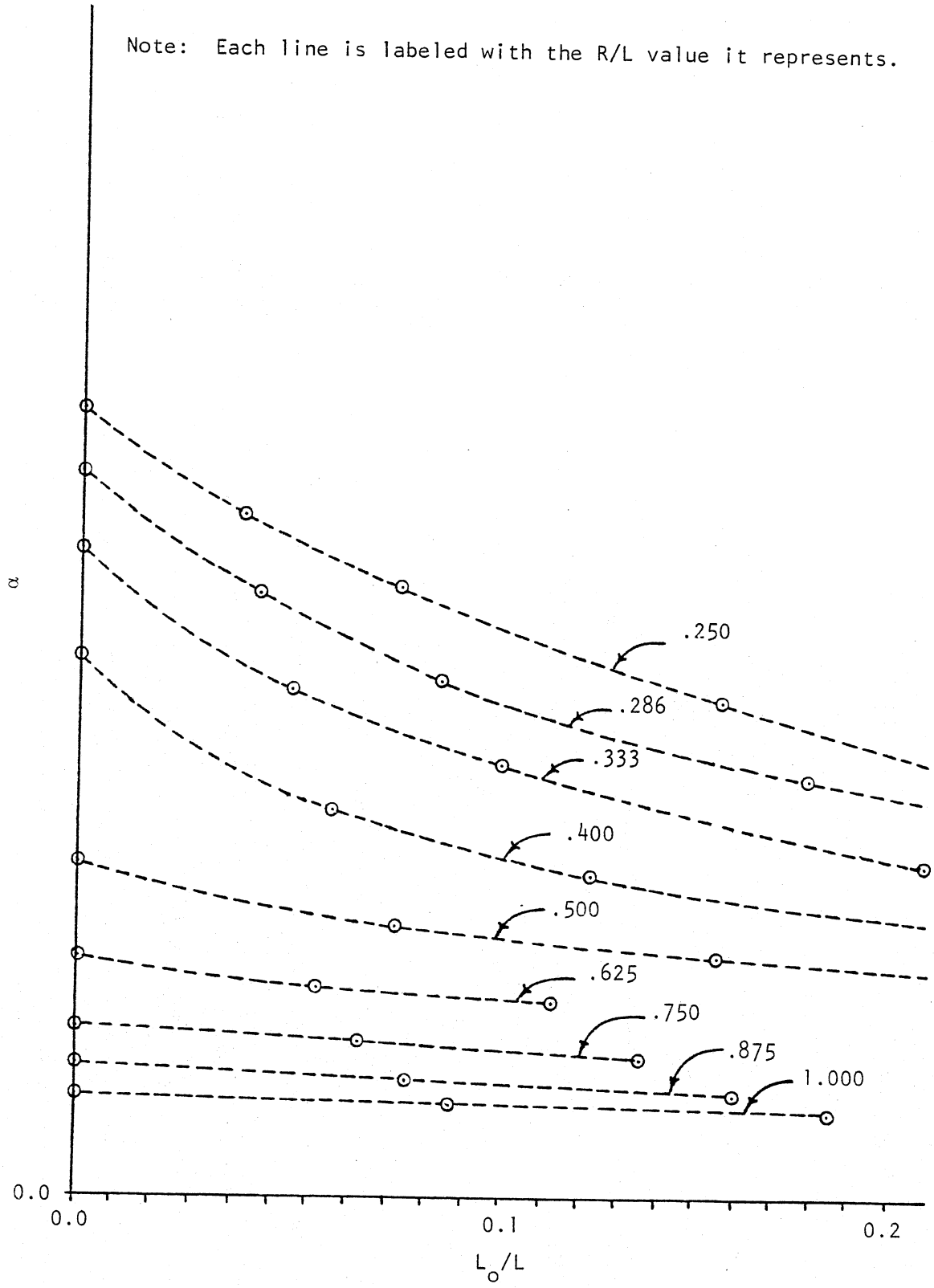

Figure 22. First Out-of-Plane Mode (α vs. L_o/L)

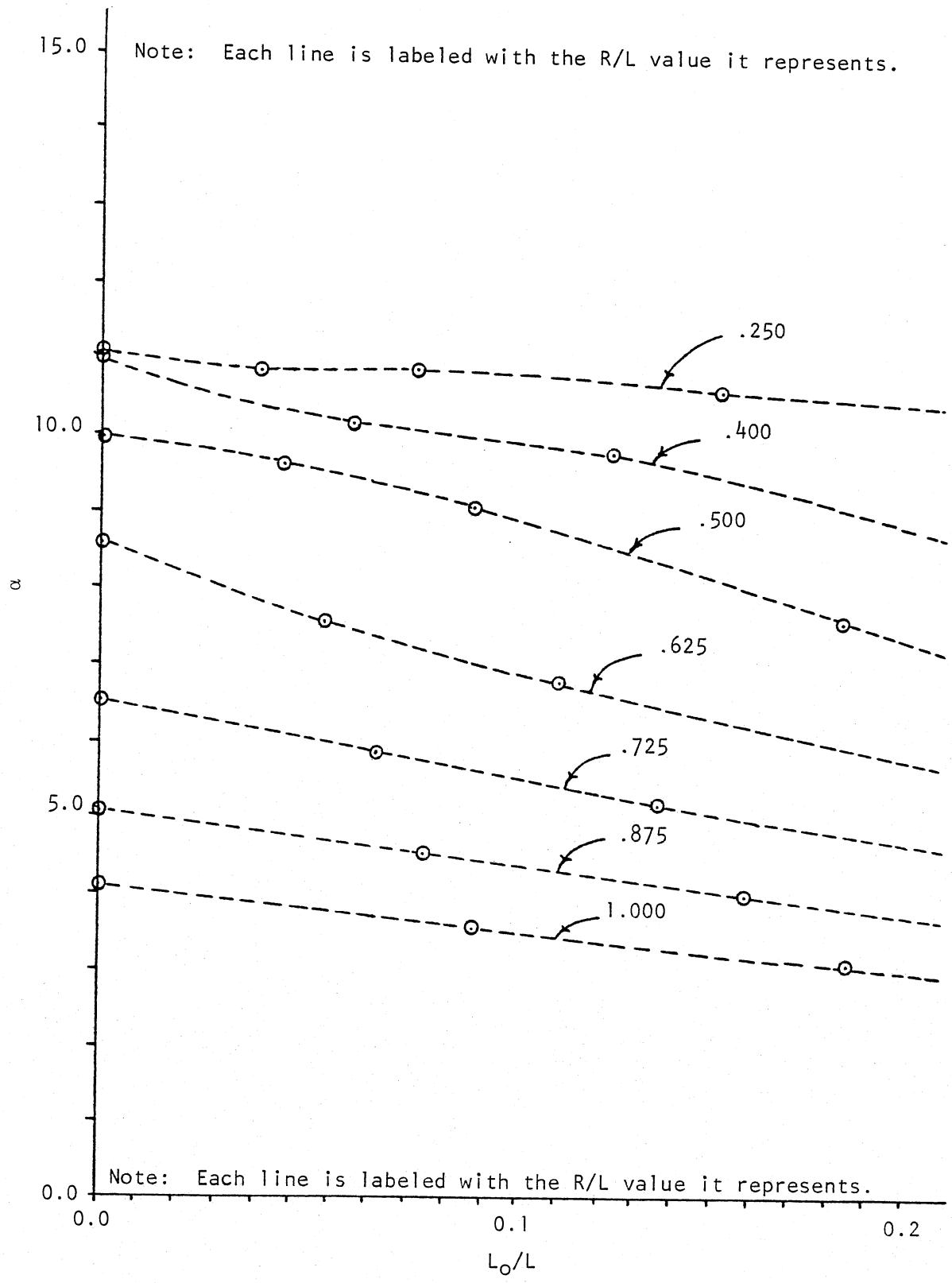

Figure 23. Second Out-of-Plane Mode (α vs. L_o/L)

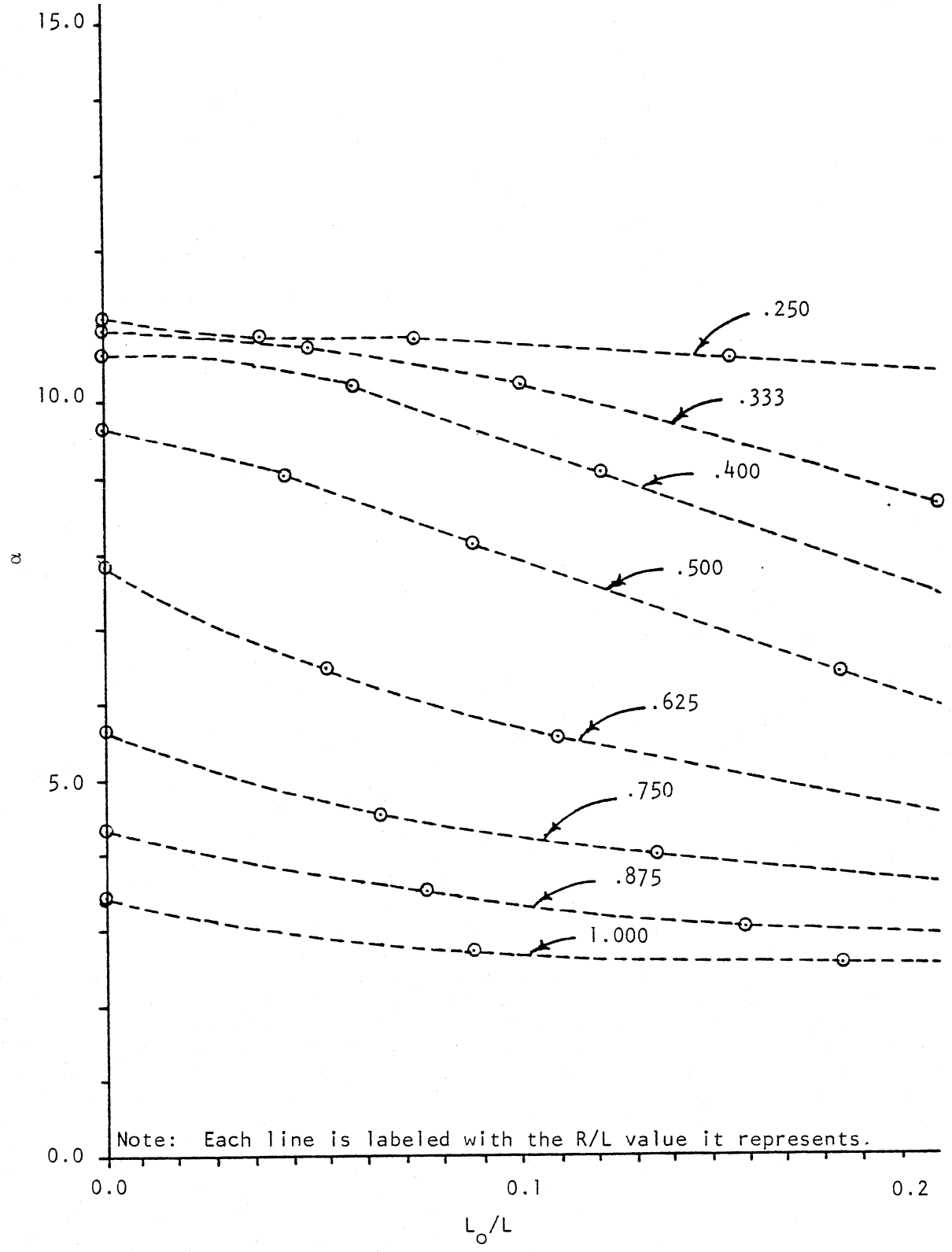

Figure 24. First In-Plane Mode (α vs. L_o/L)

When trying to excite the first out-of-plane mode, it could not be excited with the electromagnets along the span lengths for R/L ranging from 1/2 to 1. But with the electromagnets placed along the semicircular section of the U-tube, the first out-of-plane mode went into resonance with ease.

The second out-of-plane mode and the first in-plane mode became difficult to excite when the span lengths and R/L approached 1. These two modes easily went into resonance when the excitation force was moved to the semicircular section of the U-tube.

Referring to Figure 12, the δ_{SL}/δ_{SS} was about 1/2 when the difficulties to excite the U-tube along the span lengths occurred. When δ_{SL}/δ_{SS} was less than 1/2, the corresponding modes could not be excited along the span lengths with the electromagnets. For the mode shapes with δ_{SL}/δ_{SS} equal to or less than 1/2, the majority of the kinetic and potential energy was in the semicircular section of the U-tube.

When a structure goes into resonance, the structure must vibrate in the mode shape of the applied natural frequency and not in some random mode shape. Therefore, with δ_{SL}/δ_{SS} less than 1/2, the excitation force applied along the span lengths did not give the semicircular section the energy needed for semicircular section to vibrate in the mode shape of the applied natural frequency. With L_{SL}/L_{SS} equal to 1/2 and the span lengths given enough energy for L_{SL} to be 1, the semicircular section would need to be given enough energy for L_{SS} to be 2. Because the semicircular section was not given the energy needed to vibrate it in the mode shape of the natural frequency, the semicircular section vibrated in a random mode shape, producing a mechanical damping effect.

CHAPTER IV

HOLZER'S METHOD

A quick study of alternative methods for finding the fundamental frequency revealed that Holzer's method could be applied to any spring-mass system. In References (1), (2), and (3), the application of Holzer's method was limited to simple systems with either bending rectilinear or angular motion. These references present a technique for solving a particular set of problems. They did not define the reason Holzer's method works. The following will explain the true significance of Holzer's method.

Holzer's method was a numerical iterative method of finding the natural frequencies of a spring-mass system. This numerical iterative search was done with two equations--the system equations and the sum of the force Equations (2) and (3). In these two equations the mass m_{ij} and stiffness k_{ij} were known. The frequency f was chosen, and the mode shape x_j and constraint reactions R were evaluated. The constraint reactions R were a function of the stiffness and the mode shape.

$$4\pi^2 f^2 [m_{ij}]\{x_j\} + [k_{ij}]\{x_j\} = 0 \tag{2}$$

$$\Sigma F = -4\pi^2 f^2 \sum_{i=1}^{\ell} \sum_{j=1}^{m} m_{ij} x_j = \sum_{k=1}^{n} R_k \tag{3}$$

The process of the iterative search begins with a chosen frequency applied to the system equation. By solving the system equation, the

chosen frequency's mode shape was determined. Then the chosen frequency and its mode shape were applied to the sum of the forces. A natural frequency was found when the sum of the forces equals the sum of the constraint reactions.

Only for a natural frequency with its mode shape does the sum of the forces equal the sum of the constraint reactions. For all other frequencies with their corresponding mode shapes, the sum of the forces does not equal the sum of the reaction at the constraints.

The system equation for the spring-mass system in Figure 25 was Equation (4). To obtain the mode shape, X_1 was set equal to 1. Then X_2 and X_3 were determined by Equations (5) and (6). The mode shape was applied to the sum of the forces, Equation (7). The sum of the forces was plotted in Figure 26. From this plot the natural frequencies of the system were determined, which were 0.754, 1.414, and 1.847 radians per second. These natural frequencies were checked with the determinant method. The results were identical.

$$\begin{bmatrix} 2-w^2 & -1 & 0 \\ -1 & 2-w^2 & -1 \\ 0 & -1 & 2-w^2 \end{bmatrix} \begin{Bmatrix} x_1 \\ x_2 \\ x_3 \end{Bmatrix} = \begin{Bmatrix} 0 \\ 0 \\ 0 \end{Bmatrix} \tag{4}$$

$$x_2 = 2 - w^2 \tag{5}$$

$$x_3 = w^4 - 4w^2 + 3 \tag{6}$$

$$-w^2 (x_1 + x_2 + x_3) + x_1 + x_3 = 0 \tag{7}$$

The sum of the moment Equation (8) can also be used in Holzer's method along with or in place of the sum of the forces. In the sum of the moments, the cross products of r_j and x_j were taken, where r_j was the

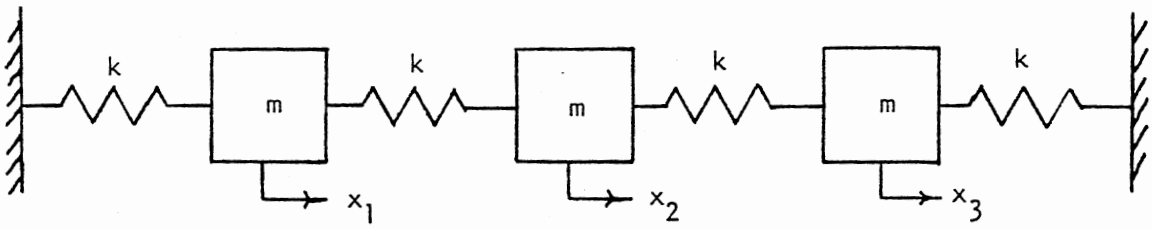

m = 1; k = 1

Figure 25. Spring-Mass System Used for an Example of Holzer's Method

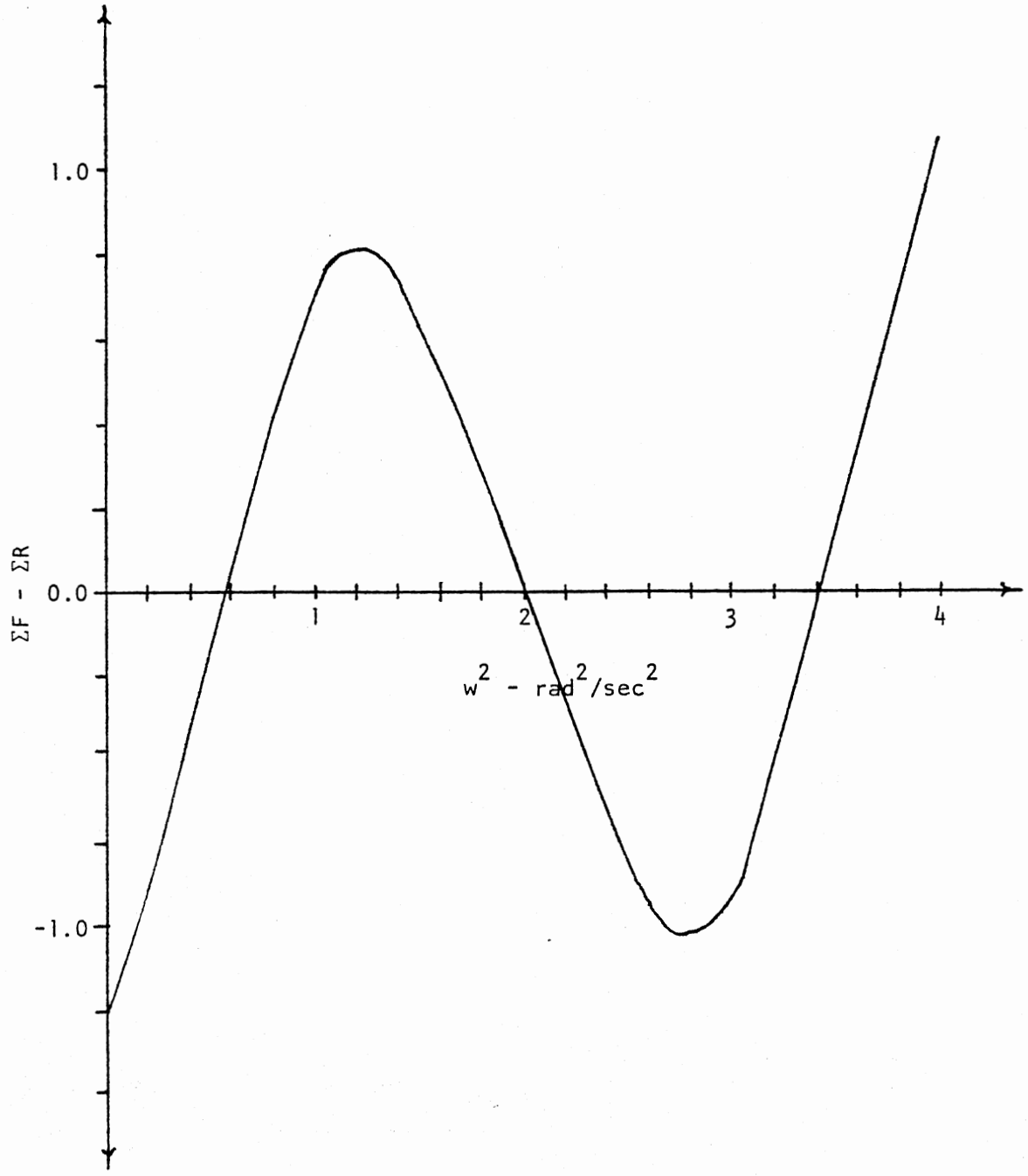

Figure 26. Sum of Forces for an Example of Holzer's Method

vector from the point, the sum of the moments was taken to the node of x_j, and T was the torsional constraint reactions. The sum of the moments can also be separated into three independent equations, because it is a vector equation and a coordinate system can have three independent rotational directions.

$$\Sigma M = 4\pi f^2 \sum_{i=1}^{\ell} \sum_{j=1}^{m} m_{ij} (r_j \times x_j) = \sum_{k=1}^{n} T_k \tag{8}$$

To compare the sum of the forces with the sum of the moments, the cantilever beam in Figure 27 was solved with Holzer's method. To simplify the problem, the cantilever beam was modeled with one element. The system equation was Equation (9). To obtain the mode shape, x_2 was set equal to one. Then x_1 was determined with Equation (10).

$$\begin{bmatrix} k_{11} - m_{11} w^2 & k_{21} \\ k_{12} & k_{22} - m_{22} w^2 \end{bmatrix} \begin{Bmatrix} x_1 \\ x_2 \end{Bmatrix} = \begin{Bmatrix} 0 \\ 0 \end{Bmatrix} \tag{9}$$

where

$$m_{11} = \frac{\mu \ell A}{2} = 0.012 \text{ lbf-sec}^2/\text{in.}$$

$$m_{22} = \frac{1}{48} m_{11} \ell^2 = 0.156 \text{ lbf-sec}^2\text{-in.}$$

$$k_{11} = \frac{12 EI}{\ell^3} = 8681.0 \text{ lbf/in.}$$

$$k_{12} = k_{21} = -\frac{6 EI}{\ell^2} = -104.1 \times 10^3 \text{ lbf}$$

$$k_{22} = \frac{4 EI}{\ell} = 1.667 \times 10^6 \text{ lbf-in.}$$

The expression for the sum of the forces and the sum of the moments were expressed with Equations (10) and (11). A plot of the sum of

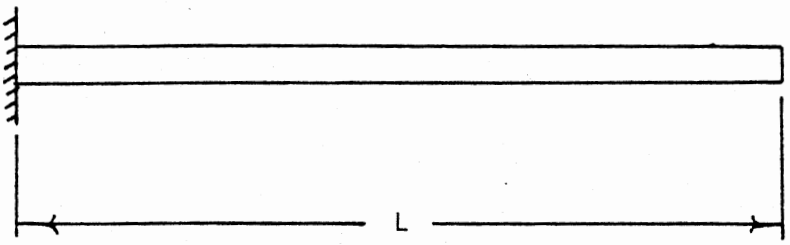

$L = 24$ in.

$E = 10^7$ lbf/in.^{2}

$I = 1.0$ in.^{4}

$\mu = 0.001$ lbf-sec^2/in.^{4}

Figure 27. Cantilever Beam Used for an Example of Holzer's Method

forces and the sum of moments is shown in Figure 28. The natural frequencies found with the sum of forces and sum of moments were the same: 66 and 533 Hz. These results were checked with the determinate method. The natural frequencies were the same.

$$k_{11}x_1 + k_{12}x_2 + m_{11}w^2x_1 = 0 \tag{10}$$

$$m_{11}w^2x_1 + m_{22}w^2x_2 + k_{12}x_1 + k_{22}x_2 = 0 \tag{11}$$

From these two examples, orderly plots were formed that crossed the zero axis only at the natural frequencies. Also, the examples showed that the acme of Holzer's method has not been reached. It can be used for any spring-mass system equation with the sum of forces or the sum of moments.

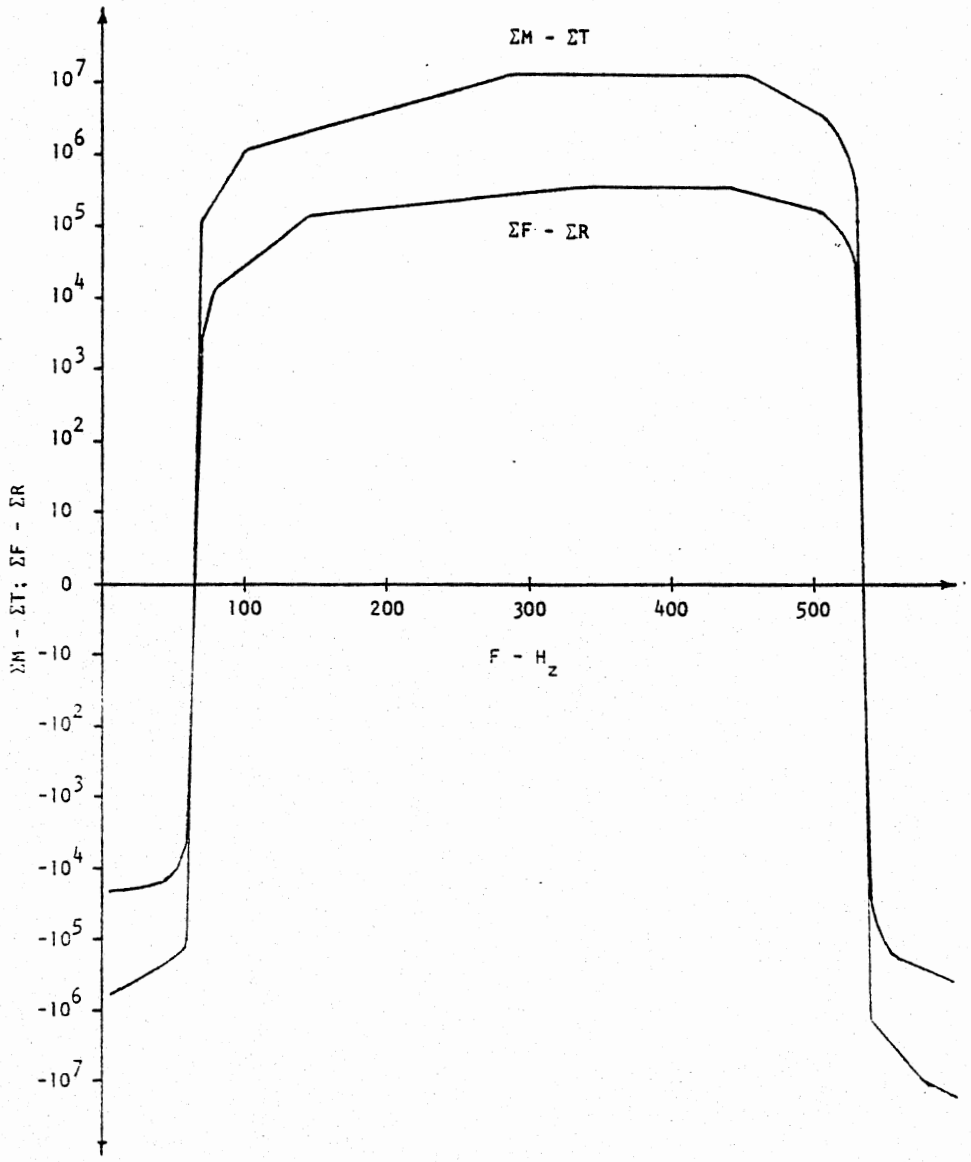

Figure 28. Sum of Forces and Sum of Moments for an Example of Holzer's Method

CHAPTER V

SUMMARY, CONCLUSIONS, AND RECOMMENDATIONS

This thesis reports an analysis of the lowest natural frequencies of heat exchanger U-tubes by numerical and experimental methods. The numerical analysis was done by modeling the U-tube with finite elements and using the generalized finite element computer program NASTRAN. In the experimental analysis, a U-tube was excited with a chosen excitation force. Then the response of the U-tube was observed.

In a search for alternative numerical methods for finding the natural frequencies of the U-tubes, a modified version of Holzer's methods was discovered.

The conclusions made from this analysis are:

1. The results from the numerical and experimental analyses of the quadruple span with ends clamped are plotted in Figures 29, 30, and 31. The maximum differences of α in the figures were less than 7 percent. The majority of the results fell directly on top of each other, which verifies that the results from the numerical and experimental analyses were accurate.

2. To put the U-tube in resonance for a given natural frequency, the excitation force must be applied in the direction of the mode shape displacements.

3. For the first out-of-plane mode of the U-tube, there is a mechanical damping effect along the span lengths.

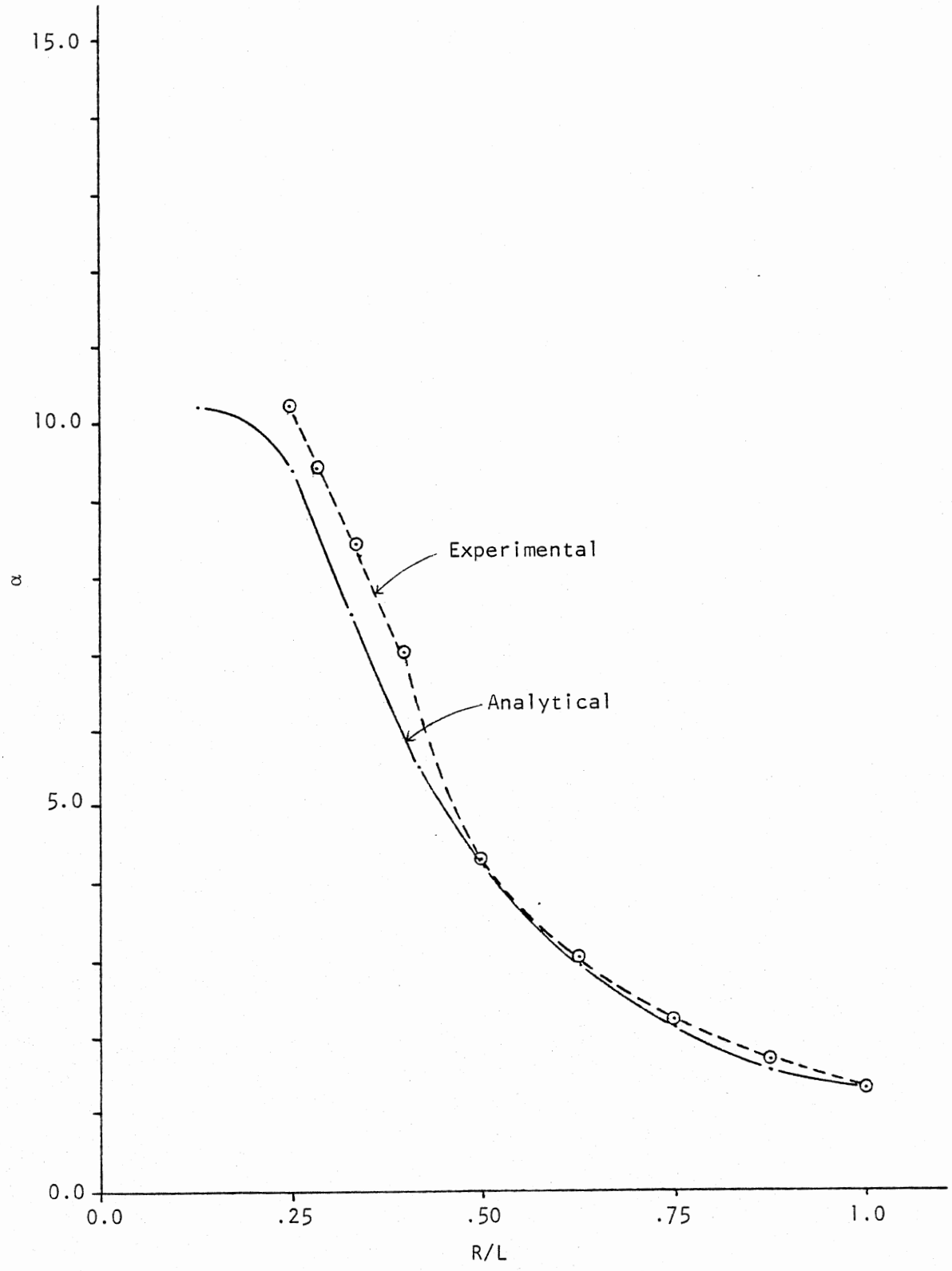

Figure 29. First Out-of-Plane Mode Quadruple Span With Ends Clamped (α vs. R/L)

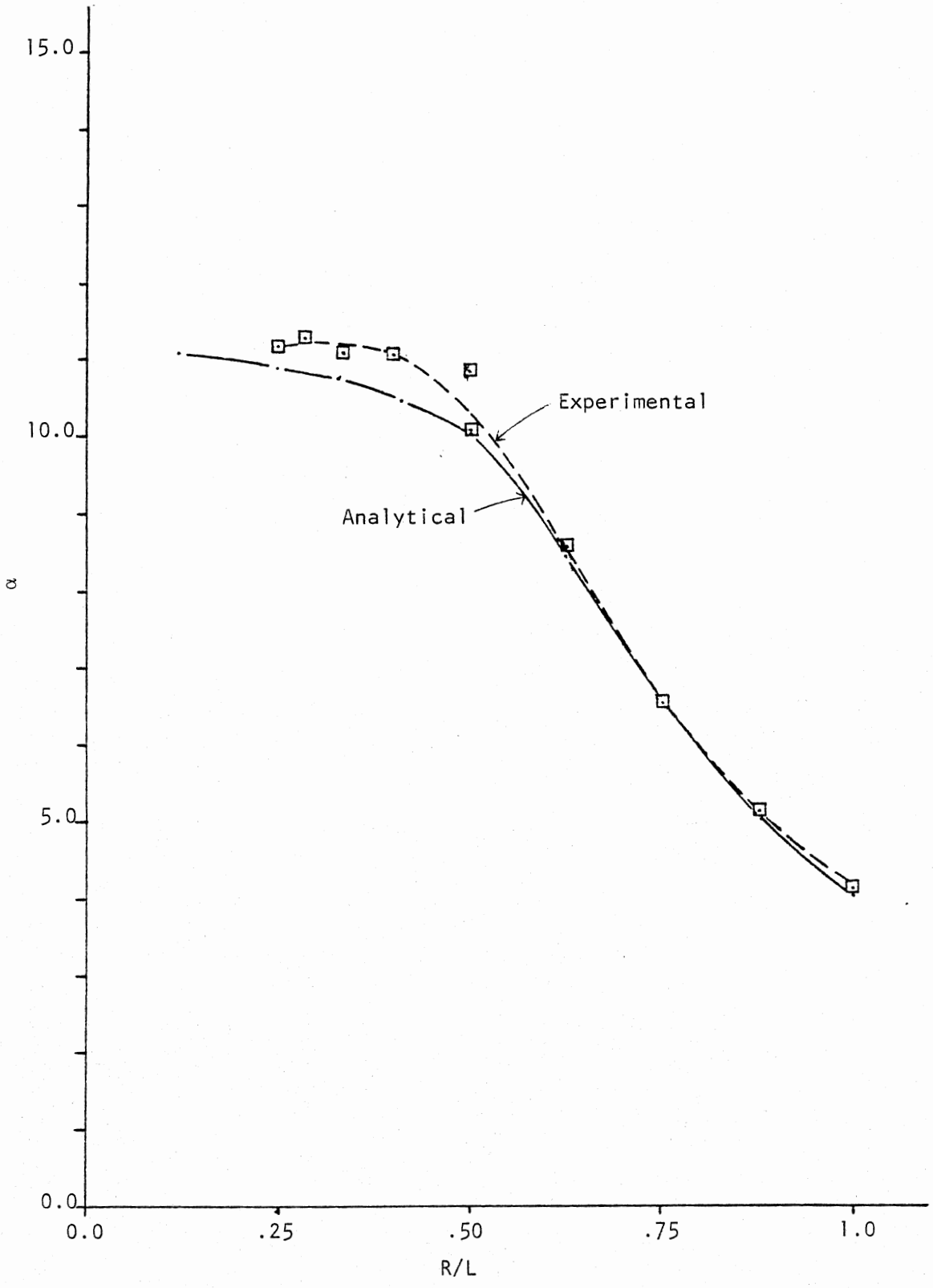

Figure 30. Second Out-of-Plane Mode Quadruple Span With Ends Clamped (α vs. R/L)

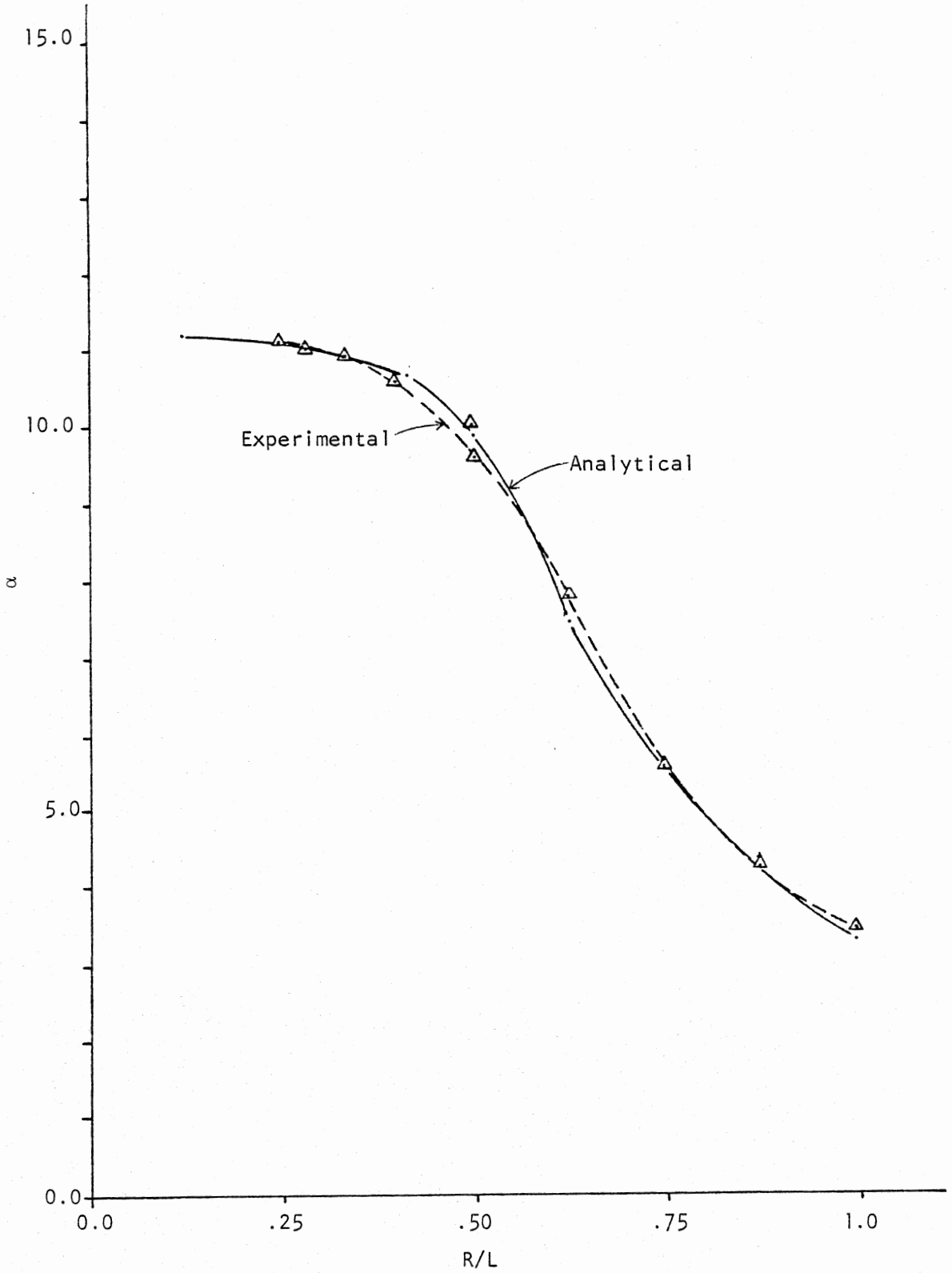

Figure 31. First In-Plane Mode Quadruple Span With Ends Clamped (α vs. R/L)

4. The natural frequencies were lowered when the overhang length is increased.

5. With the excitation frequency being a natural frequency, the U-tube must resonate in the mode shape of the natural frequency.

6. The modified version of Holzer's method can be applied to any spring mass system.

Recommendations for continuing the analysis of the lowest natural frequencies of heat exchanger U-tubes are:

1. Conduct an analysis of the mechanical damping effects of the first out-of-plane mode with continuous system modeling programs.

2. Analyze the change of natural frequencies for the maximum kinetic and maximum and maximum potential energy along the span lengths versus the semicircular section.

3. Analyze the effects of using different span lengths for all of the span lengths of a multispan configuration.

BIBLIOGRAPHY

(1) Thompson, William T. Theory of Vibration With Applications. Englewood Cliffs, N.J.: Prentice-Hall, 1972.

(2) Steidel, Robert E., Jr. An Introduction to Mechanical Vibrations. 2nd Edition. New York: Wiley and Sons, 1979.

(3) Tse, F. S., I. E. Morse, and R. T. Hinkle. Mechanical Vibrations Theory and Application. 2nd Edition. Boston: Allyn and Bacon, Inc., 1978.

(4) Lowery, R. L., and P. M. Moretti. Heat Exchanger Tube Vibration Characteristics in a No Flow Condition. Final Report. White Plains, N.Y.: Tubular Exchanger Manufacturers Association, 1973.

(5) Tauchert, T. R. Energy Principles in Structural Mechanics. New York: McGraw-Hill, 1974.

(6) Fazely, A. "Analysis of Lowest Natural Frequency in Heat-Exchanger U-Tubes." (M.S. report, Oklahoma State University, Stillwater, Oklahoma, 1977.)

(7) Lee, L. S. S. "Vibrations of an Intermediate Support U-Bend Tube." ASME Paper No. 73-DE-H, 1973.

APPENDIX A

THREE NATURAL FREQUENCIES BY NUMERICAL ANALYSIS

The lowest three natural frequencies from the numerical analysis with NASTRAN are tabulated below. Along with the natural frequencies are the corresponding values of α, where α is the dimensionless value in Equation (1). For the configuration, refer to Figure 1.

R/L	First-Out-Of-Plane Mode		Second-Out-Of-Plane Mode		First-In-Plane Mode	
	$f - H_z$	α	$f - H_z$	α	$f - H_z$	α
Single Span Configuration						
1/8	170.1	9.72	215.5	12.31	232.7	13.30
1/4	150.3	8.59	198.4	11.34	216.3	12.36
1/3	121.1	6.92	189.8	10.85	204.9	11.71
5/12	91.3	5.22	179.9	10.28	189.3	10.82
1/2	69.1	3.95	166.4	9.51	166.1	9.49
5/8	47.7	2.72	137.9	7.88	125.4	7.17
3/4	34.7	1.98	108.2	6.18	93.6	5.35
7/8	26.4	1.51	84.7	4.84	71.7	4.10
1	20.7	1.18	67.5	3.85	56.5	3.22
Double Span Configuration						
1/4	158.2	9.04	184.1	10.52	181.9	10.39
1/2	72.1	4.12	168.9	9.65	169.4	9.68
3/4	35.8	2.04	112.7	6.44	96.6	5.52
1	21.3	1.22	69.5	3.97	58.0	3.31
Triple Span Configuration						
1/4	160.1	9.14	179.2	10.24	181.9	10.39
1/2	72.3	4.13	169.8	9.70	169.4	9.68
3/4	35.9	2.05	113.4	6.48	96.6	5.52
1	21.3	1.22	69.7	3.98	58.0	3.31
Quadrupal Span Configuration						
1/4	161.9	9.25	177.0	10.12	178.4	10.20
1/2	72.4	4.14	177.0	10.12	169.4	9.68
3/4	35.9	2.05	113.4	6.48	96.6	5.52
1	21.3	1.22	69.7	3.98	58.0	3.31
Quadrupal Span With Ends Clamped Configuration						
1/8	178.9	10.22	194.7	11.13	196.48	11.23
1/4						
1/3	131.84	7.53	187.8	10.73	192.1	10.98
5/12	97.6	5.58	183.8	10.51	187.2	10.7
1/2						
5/8	50.3	2.87	147.4	8.42	130.6	7.46
3/4						
7/8	27.9	1.59	88.1	5.04	73.7	4.21

APPENDIX B

RATIO OF MAXIMUM DEFLECTIONS

Tabulated below is the maximum deflection of the span lengths divided by the maximum deflection of the semicircular section (L_{SL}/L_{SS}) from the numerical analysis. For the configuration, refer to Figure 1.

R/L	First-Out-Of-Plane Mode L_{SL}/L_{SS}	Second-Out-Of-Plane Mode L_{SL}/L_{SS}	First-In-Plane Mode L_{SL}/L_{SS}
Single Span Configuration			
1/8	2.469	11.598	13.230
1/4	.933	4.505	5.10
1/3	.501	2.970	3.062
5/12	.310	2.025	1.834
1/2	.217	1.366	1.08
5/8	.146	.746	.575
3/4	.107	.466	.380
7/8	.083	.291	.333
1	.065	.256	.232
Double Span Configuration			
1/4	.879	6.031	8.21
1/2	.179	1.326	1.044
3/4	.087	.388	.323
1	.053	.210	.193
Triple Span Configuration			
1/4	.861	7.547	11.05
1/2	.175	1.314	1.023
3/4	.085	.376	.316
1	.052	.205	.190
Quadrupal Span Configuration			
1/4	.853	9.881	13.66
1/2	.175	1.309	1.009
3/4	.085	.374	.315
1	.052	.204	.190
Quadrupal Span With End Clamped Configuration			
1/8	2.414	17.50	14.33
1/4	.844	5.464	7.14
1/3	.422	3.205	3.940
5/12	.256	2.000	1.895
1/2	.180	1.251	.953
5/8	.122	.607	.469
3/4	.089	.3708	.314
7/8	.069	.264	.238
1	.055	.203	.190

APPENDIX C

THREE NATURAL FREQUENCIES BY EXPERIMENTATION

Tabulated below are the lowest three natural frequencies from the experimentation. For the measurements taken, R/L ranged from 1/4 to 1, and L_o ranged from 0 to 24 inches. Along with the natural frequencies are the corresponding values of α, where α is the dimensionless value in Equation (1). All configurations used in the experimentation were quadrupal span with ends clamped.

Overhang Length L_o	First-Out-Plane f	First-Out-Plane α	Second-Out-Plane f	Second-Out-Plane α	First-In-Plane f	First-In-Plane α
R/L = 1/4 L = 48" R = 12"						
0"	35	10.2	38	11.1	38	11.1
2"	30	8.8	37	10.8	37	10.8
4"	27	7.9	37	10.8	37	10.8
8"	22	6.4	36	10.5	36	10.5
12"	18	5.3	35	10.2	34	10.0
16"	0	0	34	10.0	29	8.5
20"	0	0	30	8.8	24	7.0
R/L = 2/7 L = 42" R = 12"						
0"	42	9.4	50	11.2	49	11.0
2"	35	7.8	47	10.5	47	10.5
4"	30	6.7	46	10.3	47	10.5
8"	24	5.4	45	10.1	45	10.1
12"	19	4.3	43	9.6	38	8.5
16"	0	0	38	8.5	30	6.7
20"	0	0	33	7.4	25	5.6
R/L = 1/3 L = 36" R = 12"						
0"	51	8.4	67	11.0	66	10.9
2"	40	6.6	64	10.5	65	10.7
4"	34	5.6	62	10.2	62	10.2
8"	26	4.3	58	9.5	52	8.6
12"	21	3.5	54	8.9	42	6.9
16"	0	0	43	7.1	32	5.3
20"	0	0	35	5.8	26	4.3
R/L = 2/5 L = 30" R = 12"						
0"	61	7.0	96	11.0	93	10.6
2"	44	5.0	88	10.1	89	10.2
4"	38	4.3	85	9.7	79	9.0
8"	28	3.2	69	7.9	58	6.6
12"	22	2.5	53	6.1	44	5.0
16"	17	1.9	46	5.3	33	3.8
20"	0	0	37	4.2	27	3.1
R/L = 1/2 L = 24" R = 12"						
0"	59	4.3	148	10.8	136	10.0
2"	48	3.5	122	8.9	113	8.3
4"	42	3.1	109	8.0	90	6.6
8"	30	2.2	81	5.9	62	4.5
12"	23	1.7	61	4.5	46	3.4
16"	19	1.4	49	3.6	35	2.6
20"	0	0	39	2.9	28	2.0

Overhang Length L_o	First-Out-Plane f	First-Out-Plane α	Second-Out-Plane f	Second-Out-Plane α	First-In-Plane f	First-In-Plane α
R/L = 1/2 L = 41" R = 20.5"						
0"	20	4.3	47	10.0	45	9.6
2"	18	3.8	45	9.6	42	9.0
4"	0	0	42	9.0	38	8.1
8"	0	0	35	7.5	30	6.4
12"	0	0	29	6.2	24	5.1
16"	0	0	25	5.3	20	4.3
20"	0	0	21	4.5	Just below 17	
R/L = 5/8 L = 32.8" R = 20.5"						
0"	23	3.1	63	8.6	57	7.8
2"	20	2.7	55	7.5	47	6.4
4"	18	2.5	49	6.7	41	5.6
8"	0	0	39	5.3	31	4.2
12"	0	0	32	4.4	25	3.4
16"	0	0	27	3.7	21	2.9
20"	0	0	0	0	0	0
R/L = 3/4 L = 27.33" R = 20.5"						
0"	23	2.2	68	6.5	59	5.6
2"	21	2.0	61	5.8	47	4.5
4"	18	1.7	54	5.1	42	4.0
8"	0	0	42	4.0	33	3.1
12"	0	0	34	3.2	26	2.5
16"	0	0	29	2.8	22	2.1
20"	0	0	24	2.3	18	1.7
R/L = 7/8 L = 23.43" R = 20.5"						
0"	24	1.7	73	5.1	62	4.3
2"	22	1.5	64	4.5	52	3.6
4"	19	1.3	56	3.9	44	3.1
8"	0	0	44	3.1	34	2.4
12"	0	0	35	2.4	27	1.9
16"	0	0	29	2.0	22	1.5
20"	0	0	24	1.7	19	1.3
R/L = 1 L = 20.5" R = 20.5"						
0"	25	1.3	77	4.1	64	3.4
2"	23	1.2	66	3.5	50	2.7
4"	20	1.1	57	3.0	47	2.5
8"	0	0	45	2.4	34	1.8
12"	0	0	37	2.0	28	1.5
16"	0	0	30	1.6	23	1.2
20"	0	0	25	1.3	19	1.0

VITA

William Terry Lester

Candidate for the Degree of

Master of Science

Thesis: ANALYSIS OF THE LOWEST NATURAL FREQUENCIES OF HEAT EXCHANGER TUBES

Major Field: Mechanical Engineering

Biographical:

Personal Data: Born in Shawnee, Oklahoma, on December 13, 1956, the son of Nova Jean and William Wilbur Lester.

Education: Graduated from Tecumseh High School, Tecumseh, Oklahoma, in May, 1975; received the Bachelor of Science in Mechanical Engineering degree from Oklahoma State University, Stillwater, Oklahoma, in 1980; completed requirements for the Master of Science degree at Oklahoma State University in May, 1982.

Professional Experience: Hughes Tool Company, Houston, Texas, 1979; teaching assistant, School of Mechanical and Aerospace Engineering, Oklahoma State University, 1980-1981.

Professional Associations: Pi Tau Sigma and American Society of Mechanical Engineers.